UNIVERSITY OF OSLO
Department of Geosciences - Meteorology and Oceanography section.

Weather routing: Sensitivity to ensemble wind and current input.

Master thesis in Geosciences Meteorology and Oceanography

Nils Melsom Kristensen

31st May 2010

Abstract

We consider the relative importance of wind and currents in the determination of optimal routes, commonly referred to as weather routing, for sailboats. Weather routing for sailboats is the process of finding the fastest route from one place to another based on wind and current information combined with information about the boats performance. In this thesis we also take into account the uncertainty in the wind and current information by making use of ensemble predictions. Our overall conclusion is that currents is a decisive factor in the determination of the fastest (optimal) routes for sailboats, and can be a decisive factor in the routing process. The wind information is extracted from met.no's ensemble prediction system LAMEPS. Each ensemble forecast is in turn used to force the ocean model ROMS to provide an ensemble of ocean currents as well. Regarding the routing, we study two different cases, one in which the boat is sailing against the wind (the upwind case) and one in which the boat is sailing with the wind from behind (the downwind case). This is repeated using each of the ensemble members as input, giving us an ensemble of possible optimal routes. We then compare the routes made with and without currents as input. For both cases, there is a reduction in sailtime of about $1 - 1.5\%$ following the route based on both wind and current input compared to the route calculated using wind as input only, given that the weather and current would develop according to the forecast. We also calculate what is referred to as the mean and median route by averaging the routes geographically. These routes are simulated for all the different weather and current ensemble members. In three out of four cases, the mean route perform better than the route suggested by the deterministic forecast. This indicates that the use of ensemble predictions may help to improve weather routing for sailboats.

Acknowledgements

First and foremost I wish to thank my supervisor Lars Petter Røed, who made it possible for me to write this thesis, for his guidance and all the interesting discussions we have had throughout the entire writing process. I also wish to thank Ann Kristin Sperrevik who helped me set up, and taught me how to run the ocean model ROMS, and was very patient to answer all my questions in times when nothing worked as I wanted it to.

A special thanks to Nick White who made the routing software Expedition available for this thesis work. Without it, it would not have been possible to perform the weather routing in this thesis.

Thanks to the Norwegian Meteorological Institute for giving me access to their models.

Thanks also to my fellow students, friends and family.

Nils Melsom Kristensen
Oslo, May 2010

Contents

Chapter 1

Introduction

We consider whether ocean currents can play a decisive role when calculating optimal routes for sailboats given uncertainties in the weather forecast.

Small variations in the current can be crucial if we consider the fact that two boats that experience a current difference of as little as 0.01 knots for one hour, will be separated by almost 20 meters. After 10 hours, the difference is 185 meters.

Sailors are a group of people who has a keen interest in weather, wind and ocean currents. The motivation for this special interest is that good knowledge about these variables are crucial for the planning of long-distance yacht-races, with regards to both safety and competitiveness. All professional, and many amateur, racing-teams today make use of sophisticated instruments and computer systems on board and ashore. Weather-routing programs are a common and important part of these systems. There are several programs available on the market. Here we have used a program called Expedition, since this was made easily available to us. The weather-routing programs use information about wind and currents as input. This information is used together with information about the boats performance to calculate the fastest route from one geographical point to another. Usually this is done with one deterministic forecast for wind, and one deterministic forecast for ocean currents. The latter is not always available, and the first question we ask is: "How important is current information in this respect?"

Due to the chaotic and complex nature of the atmosphere, the weather-models produce forecasts of varying uncertainty. When the forecast is uncertain, it will result in routing based on data that does not represent the true state of the atmosphere and the ocean ("garbage in, garbage out"-principle), and one risks ending up in a unfavourable position on the

course, and being passed by competitors.

A major part of the present study is therefor devoted to studying what to do in a situation with an uncertain forecast. Our approach is to use an ensemble of atmospheric forecasts to get several equally possible realizations of how the weather is going to develop. These forecasts are then used to force an ocean model, thereby creating an ocean ensemble as well. This gives us valuable information whether small changes in the atmospheric forcing produces different developments in the ocean model forecast, which in turn leads to different routing suggestions. If for instance the ensemble predictions of the wind gives a large spread in the individual routes, then adding the current information may result in a decrease of this spread. During this work, a number of other relevant questions came up. The two most important are: 1) "Is there really a need for an ensemble for the ocean currents, or is one deterministic forecast sufficient?" 2) "How to best make use of weather and current ensembles in the routing process (i.e. choosing one route based on the ensemble of routes)?"

The thesis is organized as follows. First we give a basic introduction to the techniques and ideas used in weather routing (Chapter 2), then in Chapter 3, we give a brief description of the concepts of chaos and predictability, ensemble prediction systems and the models we have used. In Chapter 4 we introduce and describe the experiments performed, and the weather situation. The results from the experiments, and the description of one possible way of utilizing ensemble prediction in weather routing follows in Chapter 5. Furthermore we offer a discussion of the results in Chapter 6, and a summary and some final remarks in Chapter 7.

Chapter 2

The basics of weather routing

The main purpose of weather routing for sailboats is to calculate the fastest route from point A to point B using the available information about wind and current. This is usually done by special computer software (routing programs). The shortest distance from point A to point B is always the rhumbline[1], so the real question in weather routing is how far from the rhumbline one is willing to go to get more favourable weather and/or current conditions. Once a deviation from the shortest course is made, one needs to maintain a higher average speed to be able to make a net gain compared to going the shortest distance.

If the weather forecast is uncertain, it is associated with a risk to deviate from the rhumbline, since the weather may not develop according to the forecast the route is based upon. If one have no information at all about how the weather is expected to develop, one normally stick to the rhumbline. Thus, weather routing is about managing risk. One has to weigh the possible gain in sailtime for a route against the risk of choosing that particular route compared to other possible routes. In Section 5.4 we look into a possible technique to minimize the risk in route selection, and to decide how far away from the rhumbline it is safe to sail when the weather forecast is uncertain.

Even though this thesis only look into weather routing for sailboats, the same techniques and ways of thinking could be applied to calculate the optimal route for other types of boats. In either case, we need information about the boats performance, and the criteria for the optimal route (e.g. fastest route, avoiding certain wave heights, fuel consumption etc.).

[1]Line drawn directly from point A to point B, following the curvature of the earth (great circle route).

2.1 Finding the optimal route

There are quite a few routing programs available for purchase, e.g. Deckman for Windows, Adrena Tactique, Seapro and Expedition. Common for them all is that they do so called deterministic routing. This means that we put the boats performance data (see Section 2.3) and information about the wind and current (see Section 2.4) into the routing program, and the program then calculates every possible route the boat can follow, and picks the fastest one.

Figure 2.1 show a very simplified way of selecting the optimal route. The area between the start and the finish is divided into a grid, and the routing program then calculates the time used between the different points on the grid, given the wind speed and direction at the points. The current vector at each point is added to the velocity vector of the boat. The resolution of the grid is quite crucial to the result of the optimal route calculations, and one would prefer to have as high optimal routing resolution as possible to get the most accurate calculation. This is to be able to resolve variations in the wind and especially the current that can vary significantly over small distances. Since an increase in optimal routing resolution results in an increase in the computation time for the optimal routes, we simply used trial and error to find the optimal routing resolution to give us realistic results within an acceptable computational time.

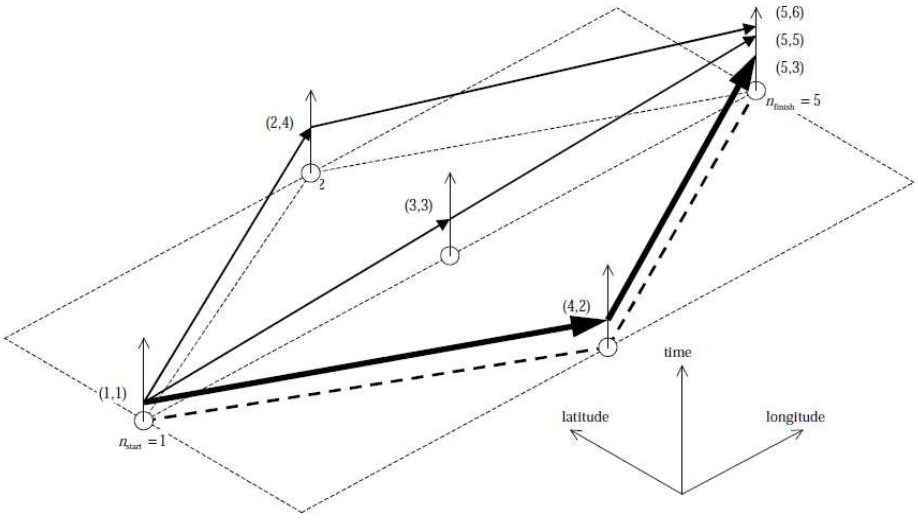

Figure 2.1: A very simplified calculation of three paths from start to finish. The bold path is the fastest - the optimal route. (Allsopp, 1998)

The alternative to this deterministic routing system would be a probabilistic system. In his thesis, Allsopp (1998), looked into the probabilistic

routing by making a stochastic routing algorithm. He concluded that the calculations was very time consuming, and there was also other factors making the technique unsuitable for implementation at the time of writing. However, his experiments showed that the route generated by the stochastic algorithm was superior to the one generated from the deterministic method when the weather forecast was uncertain.

Nordborg (2007) concluded in his master thesis that small variations in the weather input created by different WRF[2] ARW[3] simulations of the same weather situation could result in large differences in the optimal routes suggested by a routing program. He did not however take into account how currents affected these routes.

The routing algorithm that calculates the routes could differ slightly from routing program to routing program, but the general technique is the same in all of them. In this thesis, all the optimal route calculations were done using Expedition[4].

Since probabilistic routing is still experimental, and has not been implemented in the routing programs, navigators use a lot of techniques to assess the uncertainty, and thereby risk, of the route they choose. The public access to ensemble weather forecasts is very limited, so the usual way of doing the route selection is to get weather data from as many weather models as possible, and to play around with these by adjusting wind speed, direction, and the speed the weather develops at (i.e. shifting the forecast in time). It is also common to use weather input from model forecasts before the most recent to see how stable the development of the weather is, or if it changes from one model run to the next (assessing forecast jumpiness/uncertainty). All the routes created from these experiments will then be subjectively analysed by the navigator, who in the end will choose the route he or she believes most in. This technique, although providing more information than just one deterministic run, is likely to be biased, and the route selected by the navigator is in most cases the one, or very close to the one, suggested by the latest model forecast.

Our approach of doing the route selection based on uncertain weather forecasts is to make use of ensemble prediction systems (EPS). By calculating optimal deterministic routes in Expedition for each ensemble member, and analyzing them, we are trying to say something qualitatively and quantitatively about the uncertainty of the optimal route, and a possible way to calculate routes with less risk than the route suggested by the deterministic forecast alone. This is a different approach than the one suggested by Allsopp (1998), but we are hoping it will prove less time consuming,

[2]Weather Research and Forecasting model
[3]Advanced Research WRF
[4]http://www.iexpedition.org

and easier to implement into the routing program itself. To calculate the geographical mean positions[5] and the geographical standard distribution[6] we used standard software that comes with MATLAB (see Figure 2.2). The sourcecode for these calculations is offered in the Appendix.

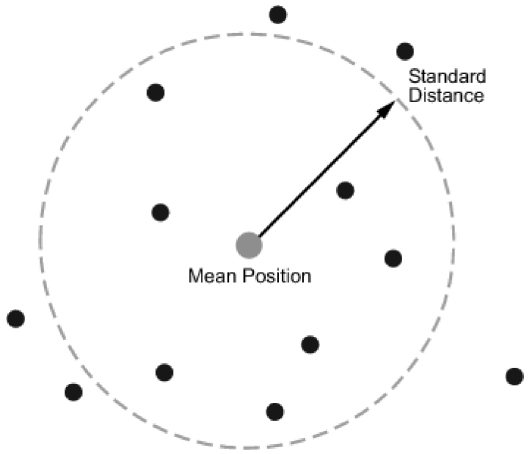

Figure 2.2: Illustration of the geographical mean position, and standard distance. The dots represent the waypoints of the different routes. Figure from MATLAB Help (Mathworks, 2007).

2.2 The course

The course we used in the experiments (see Figure 2.3) starts at the northwest corner of The Netherlands in position 53 °06.579N 004 °43.734E. The finish is just west of the Torbjørnskjær lighthouse off the coast of Norway in position 59 °00.606N 010 °45.529E. The compass course along the rhumbline from start to finish is 027 ° when going north and 207 ° going south. The distance is 407.23 nautical miles. The course was run for all the experiments in both forward and reverse direction, thereby giving us a upwind[7] and a downwind[8] case, respectively.

This course has elements of both offshore and near coastal sailing, and passes through areas of different ocean current regimes (i.e. tidally driven oscillations and density driven coastal currents).

[5] `http://www.mathworks.com/access/helpdesk/help/toolbox/map/ref/meanm.html`

[6] `http://www.mathworks.com/access/helpdesk/help/toolbox/map/ref/stdist.html`

[7] Upwind: When the wind angle relative to the boat is less than 90 °.

[8] Downwind: When the wind angle relative to the boat is more than 90 °.

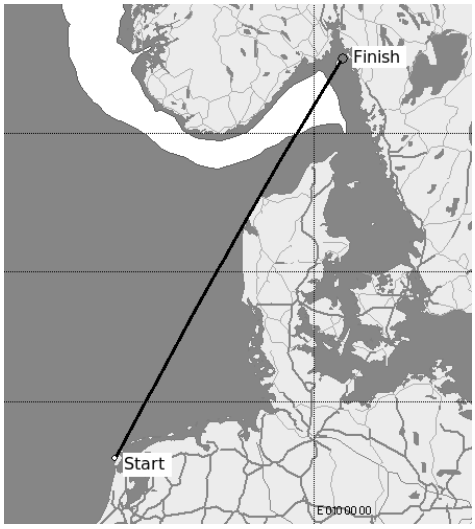

Figure 2.3: Map showing the course.

2.3 Boat performance

To be able to predict the position of the boat at a given time, given certain wind and ocean current conditions, we need to know the boats performance. This information is commonly known as polars. The polars give the boatspeed for a given wind speed and wind angle (see Figure 2.4), and can be plotted as a polar-diagram, that gives a graphical presentation of a yachts performance (see Figure 2.6).

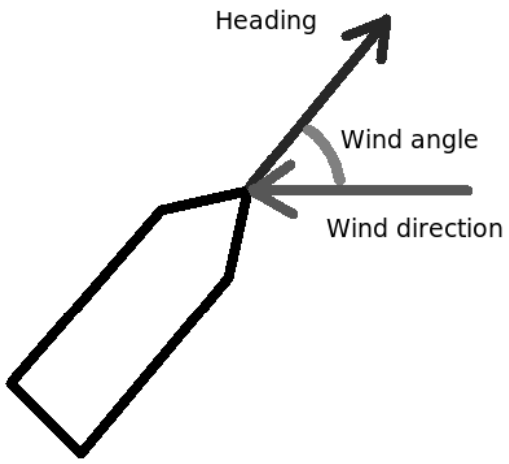

Figure 2.4: Wind angle relative to the boat.

2.3.1 The Cookson 50

Since the routing depends on the boats performance we have to use a specific boat for our purposes. The boat we used is a 'Cookson 50' (see figure 2.3.1), a fast 50 foot racing sailboat designed by Bruce Farr. The performance of the boat at different wind speeds and wind angles, are given by the polar diagram in Figure 2.6. We found it practical to use this boat since I sail as navigator on board one of these boats, and therefore have access to all performance data regarding the boat.

Figure 2.5: 'Cookson 50' sailboat. Image available from `http://www.sailinganarchy.com/fringe/2007/images/CHIEFTAIN.jpg`

2.4 GRIB-files

The weather data that is going into the routing-software need to be on a certain format, namely the GRIB-format[9]. This data-format is widely used in the sailing world because of its very good properties of storing large amounts of weather data in very small file-sizes. This is very practical since weather-data on sailboats is often downloaded trough low-bandwidth-systems (such as satellite phones or other mobile phone connections).

The GRIB-files can contain all atmospheric and ocean variables, e.g. precipitation, MSLP[10], wind, humidity, temperature, current, salinity, sea surface temperature and so on. The GRIB-files used in this thesis only include

[9] WMO standard. Abbreviation for 'GRIdded Binaries'
[10] Mean Sea Level Preassure

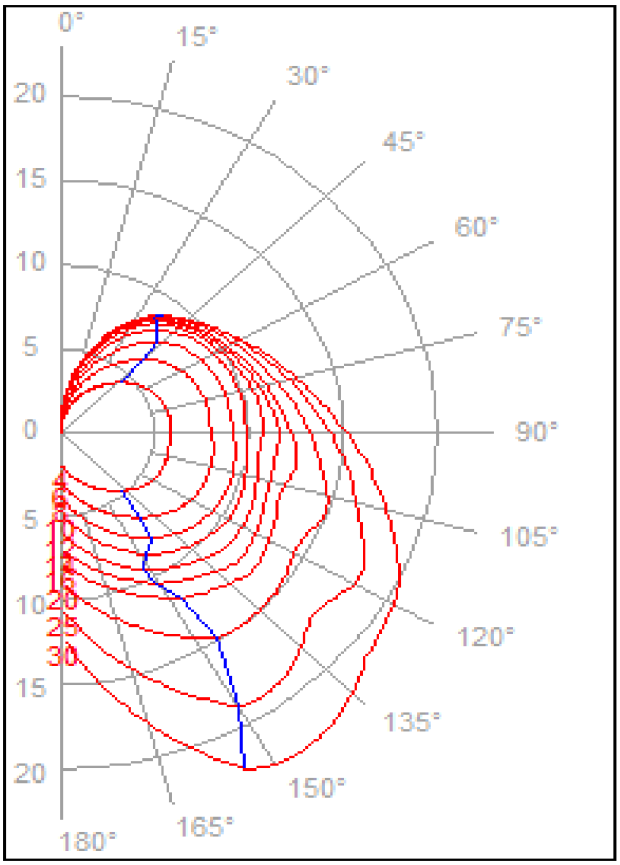

Figure 2.6: Polar diagram for the Cookson 50: Wind speed are the red numbers written on the left side of the figure. The grey numbers on the left are boatspeed, and the grey numbers written in the arc on the right are wind angle relative to the boat (see Figure 2.4). The red lines indicates the optimal speed of the boat at given wind angle and wind speed.

the u- and v-component of the wind at 10 meter height, and the u- and v-component of the current at 2 meter depth[11], as these are the only variables used in the route calculation.

[11]The draft of the boat used is 3.5 meters, so we feel that the 2 meter current will give the best representation of the forces the boat will be subject to

Chapter 3

Method

Our approach requires input from an ensemble prediction system. In our experiments we have used the weather forecasts from the operational ensemble prediction system (EPS) at the Norwegian Meteorological Institute (met.no) called LAMEPS. We also used this EPS forecast to force the ROMS ocean model to create an ocean forecast ensemble.

3.1 Ensemble prediction systems

Mathematically speaking, weather forecasting belongs to the class of problems called initial value problems. Already Wilhelm Bjerknes in his famous 1904 paper (Bjerknes, 1904) visualize weather forecasting as such a problem. Thus given the exact state of the atmosphere at a given time, and knowing the mathematical formulation of the physical laws that governs the evolution of the atmosphere we are able to calculate what the state of the atmosphere is at a later time. This is referred to as a deterministic forecast.

Thus knowing the exact initial state is critical, because even small errors in the initial state will grow in time, and the model forecast starts to deviate from the true state of the atmosphere. At a certain point the model would be no better than a random state of the atmosphere. Because of this behaviour, it is crucial to have the best possible initial conditions for our weather models to be able to predict the weather forward in time. Simplifications and error in the models themselves is another source of forecast error (Buizza, 2000). The same concept of course applies to the ocean.

It was discovered by Lorenz (1965) that even if we have a perfect model, and know the exact state of the atmosphere, we still would not be able to predict the weather much more than two weeks into the future.

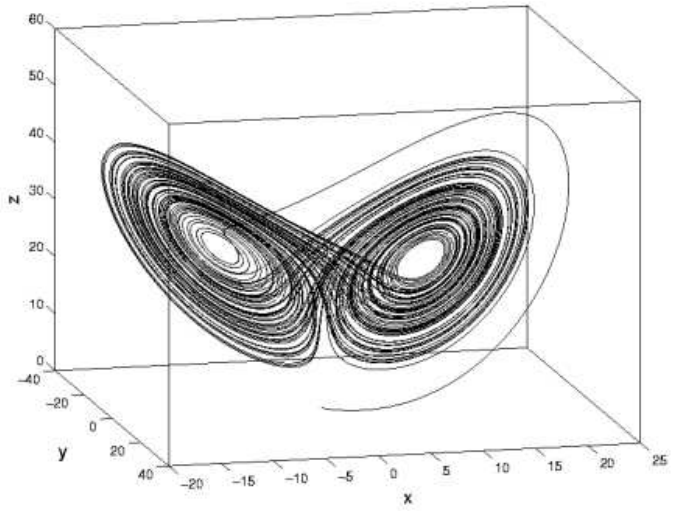

Figure 3.1: The Lorenz attractor in three dimensional phase space. (Image available from `http://complex.upf.es/~josep/lorenzatt.jpeg`)

In 1963 (Lorenz, 1963) considered a simple system of equations (3.1) given by

$$\begin{aligned} \frac{dX}{dt} &= -\sigma X + \sigma Y \\ \frac{dY}{dt} &= -XZ + rY - Y \\ \frac{dZ}{dt} &= XY - bZ \end{aligned} \tag{3.1}$$

The values of the constants in equations (3.1) was chosen by Lorenz (1963) to be $\sigma = 10$, $b = 8/3$ and $r = 28$. These are values that will give the model a critical dependence on initial conditions for X, Y and Z. There are three degrees of freedom (three dimensions), and the lines in Figure 3.1 will at no time pass through the same point in the three dimensional phase space[1].

The two blank areas within the "wings of the butterfly" in Figure 3.1, are known as strange attractors. This means that the solution of equations (3.1) will converge towards the attractor, but at some point, the solution will start to converge towards the other attractor instead (Kalnay, 2003). It actually "flip-flops" between the two attractors independent of initial state. Thus regardless of the initial condition of X, Y and Z it never ends up in either of the stationary points or attractors. If we regard the two wings as

[1]Dimension of phase space is equal to the number of degrees of freedom in the model. Phase space spans all the different solutions the model can have.

two different regimes, e.g. one warm and wet and one cold and sunny, then we can try to predict the regime instead of the exact weather one day, i.e. the exact position in the phase space at time t (Buizza, 2000).

This is where ensemble forecasting comes into the picture. Perturbed initial conditions (ICs) will result in the forecast spanning different solutions, i.e. possible developments of the weather, due to errors in the ICs (the analysis). These errors in the ICs comes because of the limited amount of data describing the state of the atmosphere at a given time (observations etc.). This method is illustrated in Figure 3.2. The ellipsoid superimposed in the Lorenz attractor represent the solutions of weather ensembles. As time evolves, the ensemble members follow the solution of the Lorenz equations, and the shape of the ellipsoid will start to deform. In the case at the top of Figure 3.2, all the ensemble members end up in the same regime after time t, which indicates good predictability. In the bottom left case the solutions stay close together for a while, but starts to spread into both wings as time progress. This means that the short term forecast is quite accurate, but the long term forecast is not that good. In the bottom right case, the solutions spread out over a very large area after a very short time. In the latter case, the forecast lose all predictability after a very short while, and the system enters chaos (Buizza, 2000).

Assessing the spread in the ensemble members at any given time, will give the user the ability to "forecast the forecast skill" (Buizza, 2000).

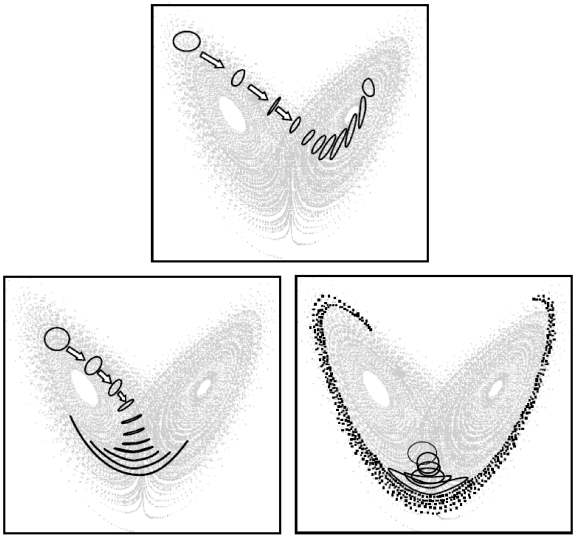

Figure 3.2: Lorenz attractor with superimposed finite-time ensemble integration. (Buizza, 2000)

The ECMWF[2] EPS that is used as initial states for the atmospheric model used in this thesis (as described in Section 3.2), use singular vectors (SVs)

[2]The European Centre for Medium-Range Weather Forecasts

to identify the initial states that makes errors in the forecast grow (Buizza, 2000). There are also other ways to generate the perturbations in the ensemble system, e.g. breeding vectors (BVs) used at NCEP[3]. The main purpose of both SVs and BVs are to identify perturbations in the ICs that will make the forecast errors grow, so the set of possible solutions (ensemble members) will span all realistic developments of the atmosphere, including the true state (se Figure 3.3) (Kalnay, 2003).

3.2 LAMEPS and HIRLAM

The HIRLAM EPS, shortened LAMEPS, is an operational ensemble prediction system at met.no. At its core is the numerical weather prediction (NWP) model HIRLAM (High Resolution Limited Area Model). As the name suggest, the HIRLAM is a limited area forecasting model with a boundary relaxation scheme. It has been developed through a collaboration between the National Meteorological Services in Denmark, Finland, Iceland, Ireland, Netherlands, Norway, Spain and Sweden. The model is a hydrostatic grid-point model and includes various parametrization schemes for sub-gridscale physical processes (Driesenaar, 2009; Unden et al., 2002). As listed on the HIRLAM webpage[4]: "The dynamical core is based on a semi-implicit, semi-Lagrangian discretisation of the multi-level primitive equations, using a hybrid coordinate in the vertical. The prognostic variables horizontal wind components u,v, temperature T, specific humidity q and linearised geopotential height G are defined at full model levels. Pressure p, geopotential height ϕ and vertical wind velocity are calculated at half levels. For the horizontal discretization, an Arakawa C-grid is used. The equations are written for a general map projection, but in practice normally a rotated lat-lon grid projection is adopted. A fourth-order implicit horizontal diffusion is applied."

LAMEPS consists of 20 ensemble members and a control run based on the Norwegian HIRLAM analysis. The ensemble members get their initial and boundary conditions from the Norwegian TEPS[5] whose perturbations are scaled and added to the HIRLAM analysis. TEPS has Europe and adjacent sea areas as target area, and is run at 12UTC and 00UTC with a forecast length of 72 hours. LAMEPS has a 6 hour time lag due to the required computation time for TEPS, and is run at 06UTC and 18UTC for +60 hours. It has a horizontal resolution of 12 km and 60 vertical levels (Aspelien, 2008). The integration domain for LAMEPS is seen in Figure 3.4.

[3]National Centers for Environmental Predictions

[4]`http://hirlam.org/index.php?option=com_content&view=article&id=64&Itemid=101`

[5]Targeted EPS, run at ECMWF

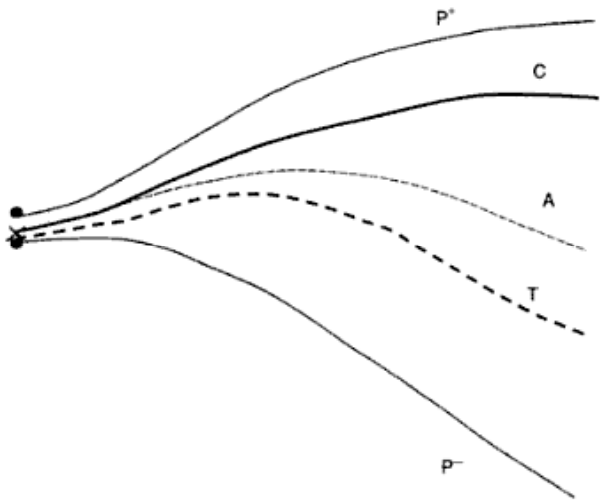

(a)

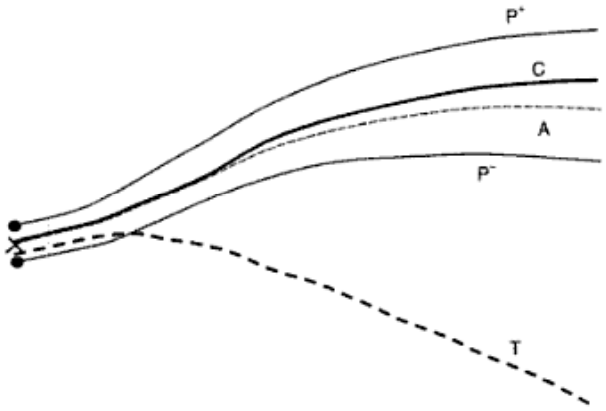

(b)

Figure 3.3: Schematic of the components of a typical ensemble (in phase space): The control forecast is labeled C, and starts from the the analysis denoted by a cross. The two ensemble members, P+ and P-, are generated trough perturbations added to, and subtracted from, the analysis. The ensemble mean is denoted by A, and the true state of the atmosphere is given by T. In panel a) we show a "good" ensemble since the true state of the atmosphere lies within the ensemble, whereas in b) the ensemble is "bad" since the true state of the atmosphere lies outside the solutions covered by the ensemble. (Kalnay, 2003).

There is not a large number of operational ensemble prediction systems in the world today, and public access to them is very limited. The alternative to using LAMEPS would be to use either the ECMWF EPS or the GFS[6] ensemble at NCEP, but both of these systems have very low spatial resolution (100km horizontal resolution for NCEP (NCEP, 1995) and 40 km horizontal resolution at ECMWF (ECMWF, 2010)). So due to its high spatial resolution, and the fact that it is made specially for our area of interest, we chose LAMEPS. In addition LAMEPS is easily available to us due to the close collaboration between the University of Oslo and the Norwegian Meteorological institute.

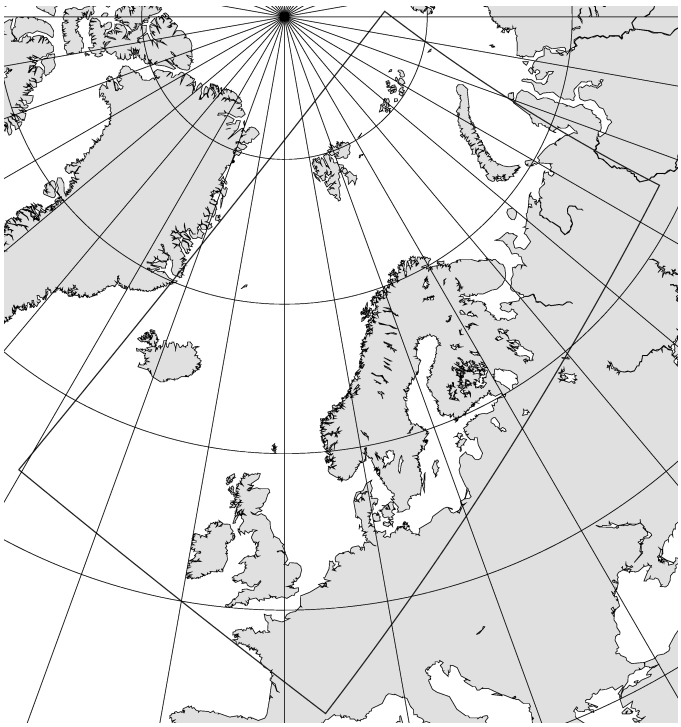

Figure 3.4: The LAMEPS integration domain.

3.3 The ROMS model

The ocean model we use is the Regional Ocean Modeling System (ROMS). This is a three-dimensional, free-surface, terrain-following numerical model that solve the Reynolds-averaged Navier-Stokes equations using the hydrostatic and Boussinesq assumptions (Haidvogel et al., 2008). ROMS has a large selection of physical and numerical options that can be specified by the user. These options are activated trough a C-preprocessor, and gives the user a selection of different turbulence closure models to parametrize

[6]Global Forecasting System

small-scale turbulent processes, various bottom boundary layer dynamics, some ecosystem modules, and a sea ice module. The model uses a S-coordinate system for the vertical coordinates (see Figure 3.6(b)). This is a nonlinear stretching version of the σ-coordinate system ($S(\sigma)$), with $-1 \leq \sigma \leq 0$, where $\sigma = 0$ is the surface and $\sigma = -1$ is the bottom. This ensures that the highest resolution is closest to the surface, which in our case is important to get the most realistic effects of the wind forcing. The Skagerrak area, for which we have run the model, is characterized by large depth fluctuations. Therefore it is advantageous to use a σ-coordinate system model compared to a z-coordinate model since this model has a better simulation of the top and bottom mixed layers. The horizontal grid is staggered using the Arakawa C-grid (see Figure 3.6(a)), and the primitive equations for the variables u, v and ρ are evaluated in different points. There is also a split-explicit time-stepping algorithm of the barotropic (fast) and baroclinic (slow) modes, where the barotropic modes has a much shorter time step than the baroclinic modes. This reduces the computational time required by the model. A thorough description of the ROMS model is given by Haidvogel et al. (2008).

The ocean ensemble members were run using ROMS version 3.2, at 4 km horizontal resolution and 32 sigma levels, for the domain shown in Figure 3.5(b). The boundary conditions (BCs) comes from the operational MI-POM[7] model at met.no covering the entire arctic region (see Figure 3.5(a)) with a horizontal resolution of 20 km. The BCs was fed into ROMS every six hours and at 8 levels. In order to get the most realistic initial conditions (ICs), and to ensure that the ROMS model was numerically stable, we did a 45 days spin-up period from MI-POM Arctic 20 km prior to the actual run of the ensemble members. The state of the model at the end of the spin-up period (2009.05.20 18UTC) was used as ICs for each of the ensemble members. Since the ICs are the same for all ensemble members, this is probably a source of bias. This will be further discussed in Chapter 6.

[7]Meteorological Institute Princeton Ocean Model

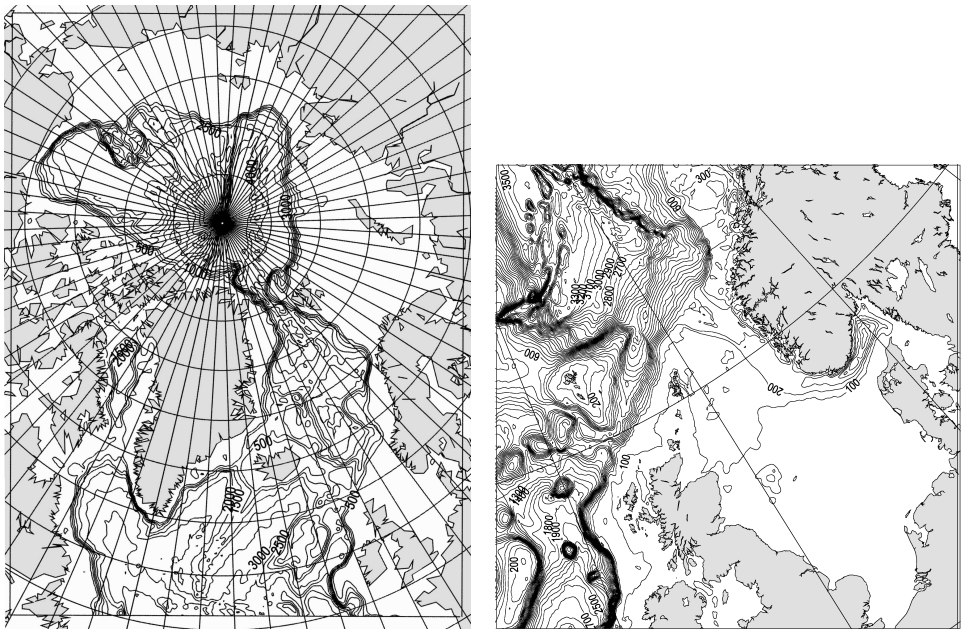

(a) **(b)**

Figure 3.5: Ocean model domains, in panel a) the MI-POM Arctic 20 km domain, and panel b) the ROMS SkagCod 4 km domain.

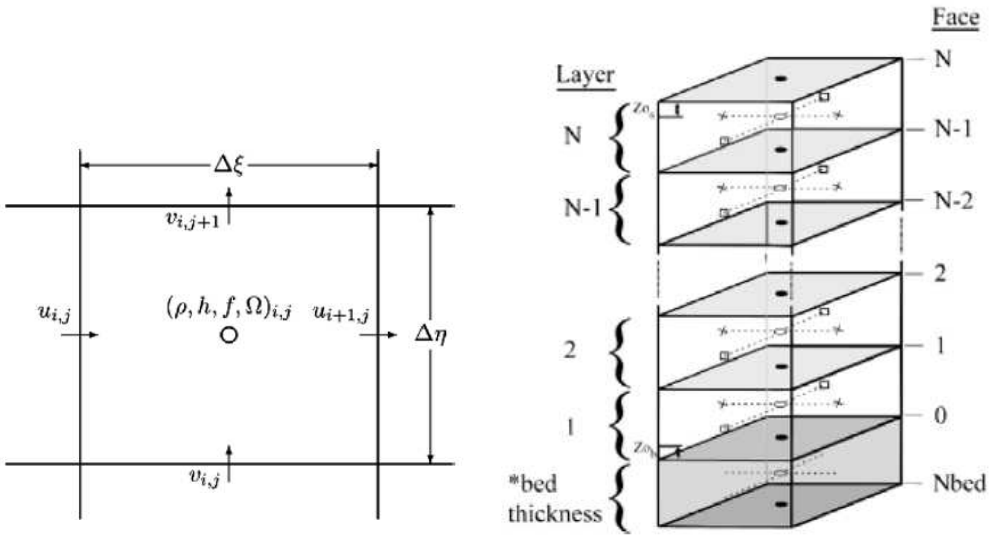

(a) **(b)**

Figure 3.6: The horizontal Arakawa C grid in panel a) and the vertical section of the ROMS grid showing placement of variables in panel b). Figure from Haidvogel et al. (2008)

Chapter 4

Experiments

4.1 Experimental setup

The experiments we perform falls basically into two classes. One set of experiments make use of deterministic forecasts only, with or without current input. The second set make use of ensemble predictions using the LAMEPS forecasts and the similar ocean ensemble predictions. For each set we run two cases, one upwind case and one downwind case. The total number of experiments are 12, as listed in Table 4.1. The downwind case use the course that starts outside the Netherlands and finish in Norway, while the upwind case run the course in the opposite direction.

When we refer to these experiments by a single number, we refer to both the upwind and downwind experiment. The deterministic set of experiments consists of Experiments 1 and 2, while Experiments 3 to 6 form the probabilistic set. The results of the deterministic experiments are based on the control forecasts. They give a first indication of how the routing is affected by adding currents, and they are used as controls in the probabilistic approach. Since the deterministic approach is the most widespread technique today, the routes suggested by these two experiments will form the basis for the evaluation of the averaged routes experiment in Section 5.4.

The set of experiments is chosen because we want to test how different combinations of wind and currents influenced the optimal routes suggested by the routing program. Experiment 3 forms the basis of which we are going to compare the experiments that include currents for the probabilistic set of experiments. Experiment 4 and 5 are closely related, and help us determine whether there is a need for an ocean ensemble, or if one deterministic forecast is sufficient. Experiment 6 gives us valuable in-

formation about the significance of small variations in the current on the suggested route when the wind input does not vary.

Experiment	Wind input	Current input	Route direction
1DN	Deterministic	None	Downwind
1UP	Deterministic	None	Upwind
2DN	Deterministic	Deterministic	Downwind
2UP	Deterministic	Deterministic	Upwind
3DN	Ensemble	None	Downwind
3UP	Ensemble	None	Upwind
4DN	Ensemble	Deterministic	Downwind
4UP	Ensemble	Deterministic	Upwind
5DN	Ensemble	Ensemble	Downwind
5UP	Ensemble	Ensemble	Upwind
6DN	Deterministic	Ensemble	Downwind
6UP	Deterministic	Ensemble	Upwind

Table 4.1: List of routing experiments in Expedition.

In all of the experiments the wind and current forecasts are fed into the routing program Expedition. The settings in Expedition are the following:

- Expedition version 7.0
- Optimal routing resolution: 10 nautical miles
- Start time: 20th of May 2009 18UTC
- Polar data: Cookson 50
- Course: See Section 2.2 on page 8

4.2 The weather situation

4.2.1 Wind, pressure and fronts

We have chosen to study a weather situation starting on the 20th of May 2009 at 18UTC (see Figure 4.1). The weather is dominated by weak pressure gradients in the target area. There is a small low pressure system forming over the northern Germany and moving northeast into the Baltic sea. There is also a small frontal system moving in from the southwest. Due to the uncertainty of the "when and where" in the development of

this small low and the passing of the frontal system, there is a significant spread in wind speed and direction within the ensemble (see Section 5.1). During the 60 hours forecast period, the wind is primarily from directions around the south and west.

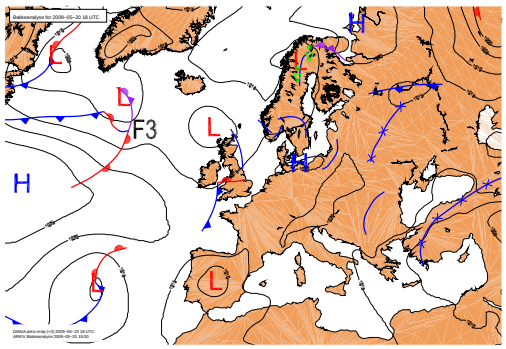

(a) Analysis 2009.05.20 18UTC (met.no)

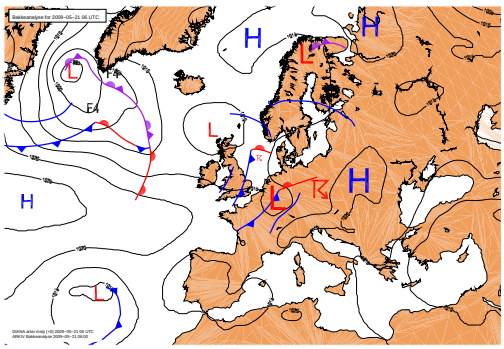

(b) Analysis 2009.05.21 06UTC (met.no)

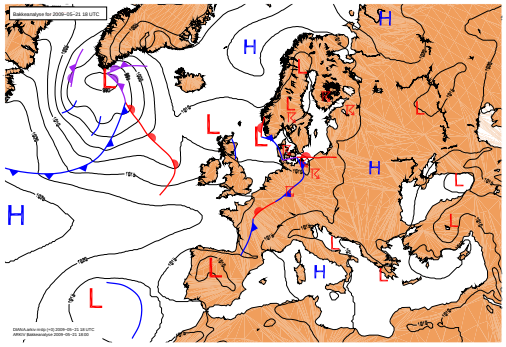

(c) Analysis 2009.05.21 18UTC (met.no)

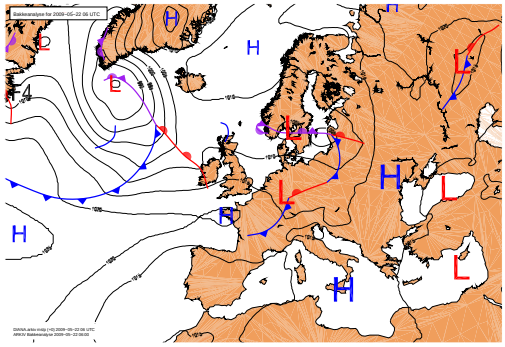

(d) Analysis 2009.05.22 06UTC (met.no)

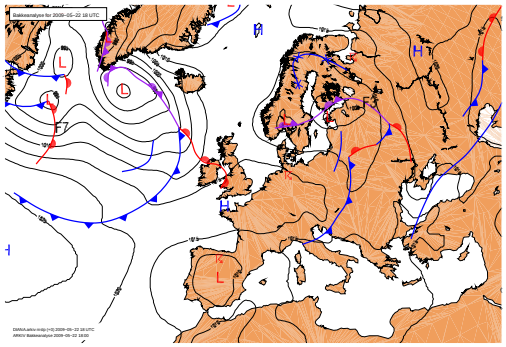

(e) Analysis 2009.05.22 18UTC (met.no)

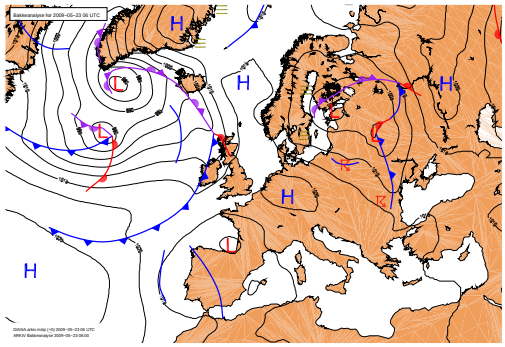

(f) Analysis 2009.05.23 06UTC (met.no)

Figure 4.1: The weather situation starting 20th of May 2009 18UTC based on the Norwegian HIRLAM analysis.

4.2.2 Ocean currents

A forecast of the current situation is displayed in Figure 4.2. This situation, in particular in the Skagerrak area in panel b), is a very typical circulation pattern with the Norwegian Coastal Current (NCC) along the south-east coast of Norway and the Jutland Current (JC) along the northern coast of Denmark (Fossum, 2006; Albretsen and Røed, 2010). Further south, along the English and Dutch coast in panel a), the current oscillates due to tidal forcing. Note also the eddy appearing at the southern tip of Norway, in the Lista area in Figure 4.2 panel b). This is a common feature in accord with earlier work on mesoscale circulation patterns in the Skagerrak (Røed and Fossum, 2004; Fossum, 2006; Melsom, 2005; Albretsen, 2007).

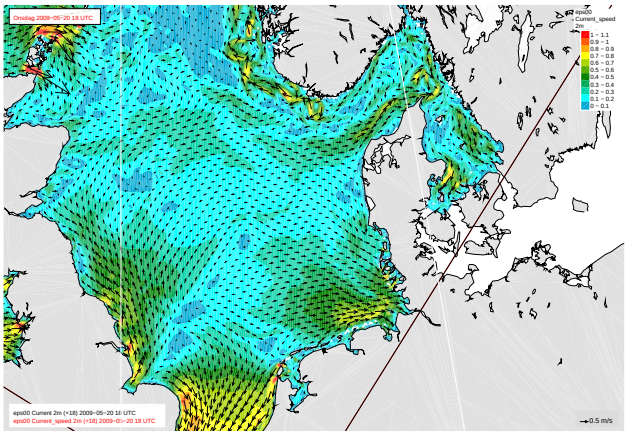

(a)

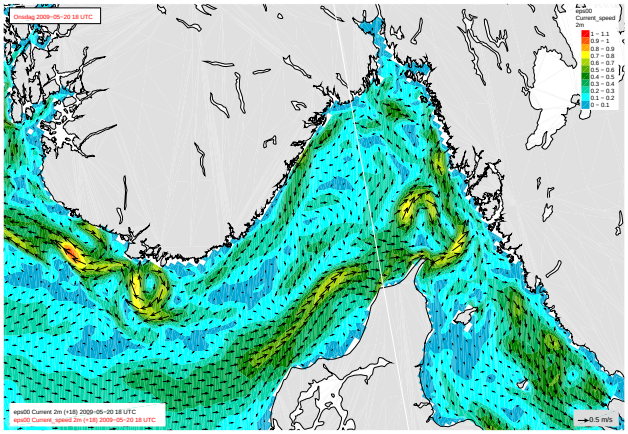

(b)

Figure 4.2: The current situation at 2009.05.20 18UTC (+00h). Panel a) show the current on the entire course, while panel b) gives a detailed picture of the Skagerrak area. Current speed is according to color scale at the top right of the figures.

Chapter 5

Results

5.1 Ensemble spread

Figure 5.2 and Figure 5.3 show the time averaged ensemble mean wind speed from LAMEPS and time averaged ensemble mean current speed from the ROMS ensemble together with the time averaged ensemble standard deviations for the entire 60 hours forecast period. The average ensemble mean wind speed in Figure 5.2a and average ensemble mean current speed in Figure 5.3a, $\overline{\langle U \rangle}_j$, in position j, is calculated using Equation 5.2, where $\langle U \rangle_{j,t}$ is the ensemble mean value in position j at time t given by Equation 5.1. N is the number of ensemble members and T is the total number of timesteps, in this case $N = 21$ and $T = 11$ (i.e. 60 hours with Δt of 6 hours).

$$\langle U \rangle_{j,t} = \frac{1}{N} \sum_{i=1}^{N} U_{i,j,t} \tag{5.1}$$

$$\overline{\langle U \rangle}_j = \frac{1}{T} \sum_{t=1}^{T} \langle U \rangle_{j,t} \tag{5.2}$$

The average ensemble standard deviation for the wind speed in Figure 5.2b and average ensemble standard deviation for the current speed in Figure 5.3b, $\overline{\sigma}_j$, in position j, is calculated using Equation 5.4, where $\sigma_{j,t}$ is the ensemble standard deviation in position j at time t given by Equation 5.3.

$$\sigma_{j,t} = \sqrt{\frac{1}{N}\sum_{i=1}^{N}\left(U_{i,j,t} - \overline{\langle U \rangle}_{j,t}\right)^2} \tag{5.3}$$

$$\overline{\sigma}_j = \frac{1}{T}\sum_{t=1}^{T}\sigma_{j,t} \tag{5.4}$$

Areas of large standard deviations are associated with areas of large ensemble spread. It is observed that the spread in wind speed is more or less uniform over the race area, while the spread in the current ensemble is more localized. Looking at Figure 5.3b, the largest spread in the current ensemble is within the Skagerrak area north of 56 °N and east of 8 °E, that is along the northwest coast of Denmark where we have the Jutland Current, along the southeast coast of Norway where we have the Norwegian Coastal Current, and north of the northern tip of Denmark, at Skagen, where there is a large eddy.

It is interesting to note that this corresponds to areas of high eddy kinetic energy as described by Røed and Fossum (2004), Albretsen (2007) and Albretsen and Røed (2010), and areas of high relative vorticity as described by Melsom (2005).

On the basis of the standard deviations for wind and current speed, we have chosen a few stations in the race area, and plotted time-series for the development of each ensemble member at these stations. The map in Figure 5.1 indicates the position for the wind and current data plotted in the figures on the following pages. In Figure 5.4 and 5.5 we observe that there is a significant spread within the wind ensemble after 6 hours, but almost no spread in the current ensemble. This is due to the tidally driven currents. In the other figures, the current is driven by a combination of the tidal forces and the atmospheric forcing. In Figure 5.6 (Station 2) there is a considerable spread in the wind speed starting from +12h. This results in a spread in current speed from +18h in Figure 5.7. The spread in current direction is very small, and is probably just due to phase differences between the tidal oscillations in the ensemble members. At Station 3, just outside Hanstholm, we find the same spread in the wind speed from +12h (see Figure 5.8). We also note the spread in current speed from +18h in Figure 5.9, but as we can see from the direction plots, the current changes little or no direction during the 60 hours period. This is evidence that the Jutland current is consistent troughout the ensemble, but it has slightly different

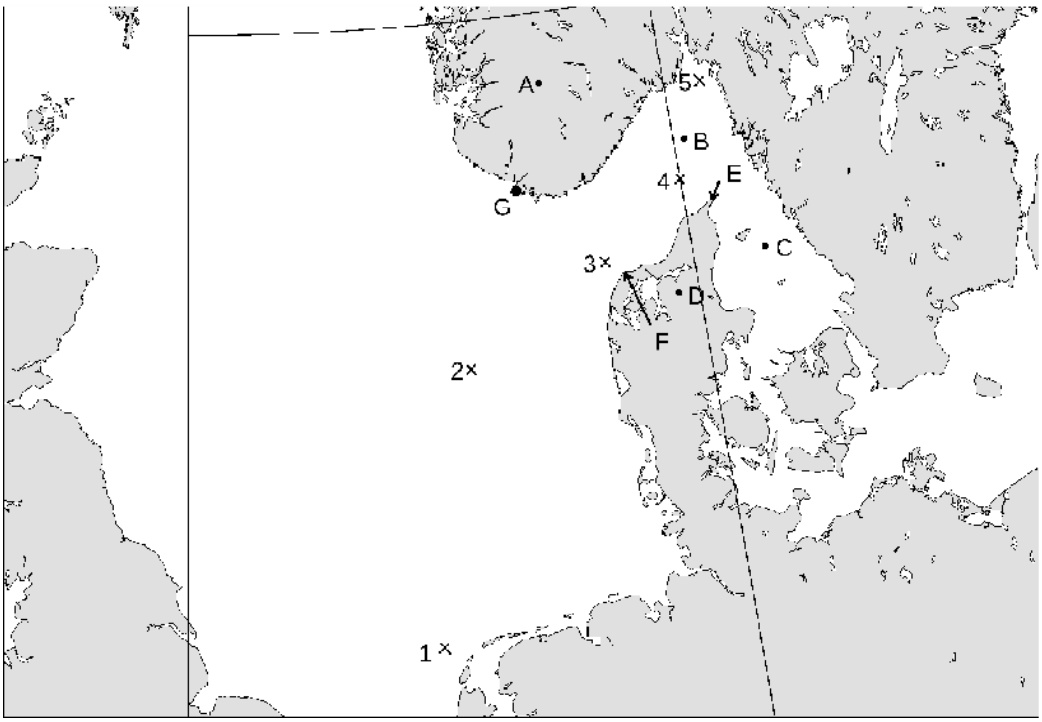

Figure 5.1: Position of the stations we display time-series for on the following pages. The letters indicate the location of geographical places and areas referred to in the text: A) Norway B) Skagerrak C) Kattegat D) Jutland E) Skagen F) Hanstholm G) Lista.

speed due to different wind forcing. Please note the large spread in current direction in Figure 5.11. This station is placed northwest of Skagen, and by looking at Figure 5.3b we see that this is an area with a large eddy and great spread in the ensemble. This spread can be observed in Figure 5.11a after about 30 hours. Station 5 is placed very close to the finish at Torbjørnskjær. The data from this station can be viewed in Figure 5.12 and 5.13. We note that the spread in both wind and current speed starts at about +18h. This is also an area of frequent eddy activity, but it seem in our case that the uncertainties in the current forecast has to do with speed more than direction.

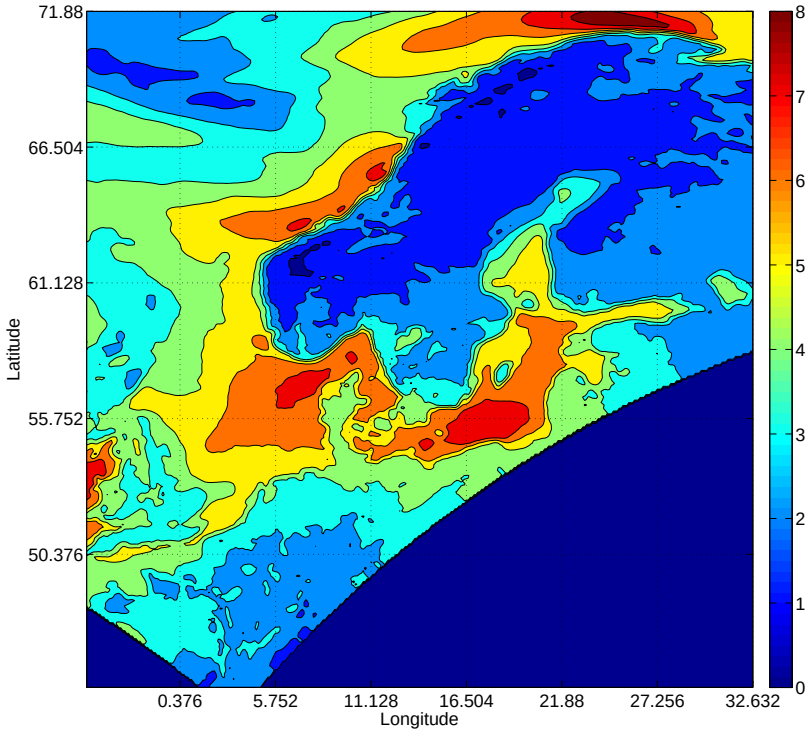

(a) Average ensemble mean 10m wind speed (m/s) over the 60 hour period.

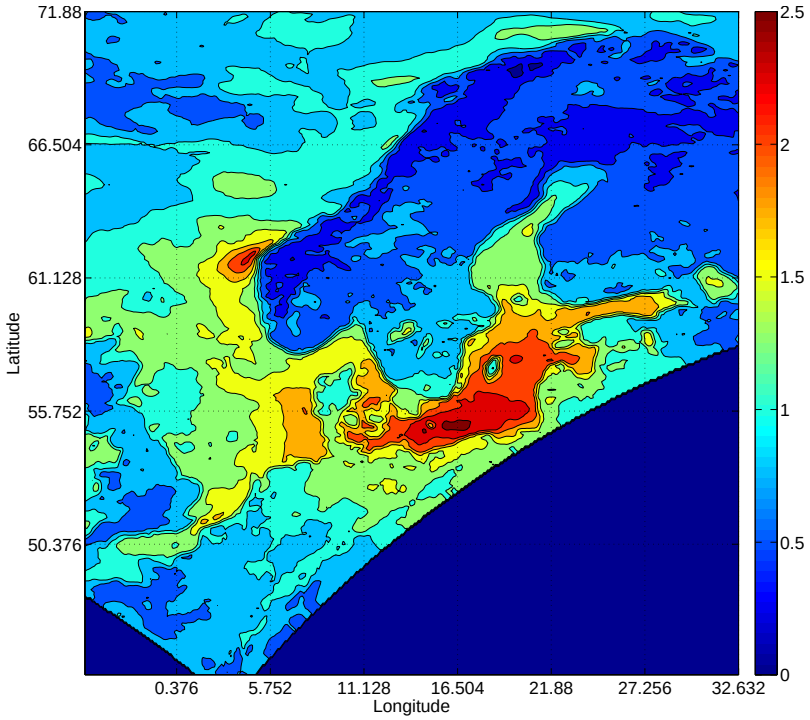

(b) Average ensemble standard deviation for 10m wind speed (m/s) over the 60 hour period.

Figure 5.2: Average ensemble mean and average ensemble standard deviation for wind speed. Areas with a large standard deviation is an indication of large ensemble spread for that area during the forecast period.

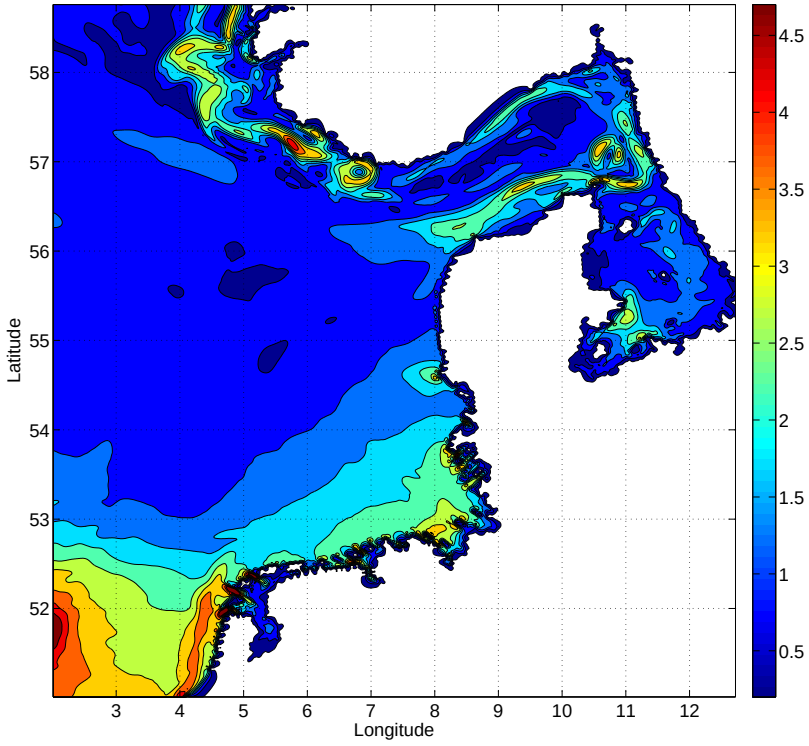

(a) Average ensemble mean 2m current speed (m/s) over the 60 hour period.

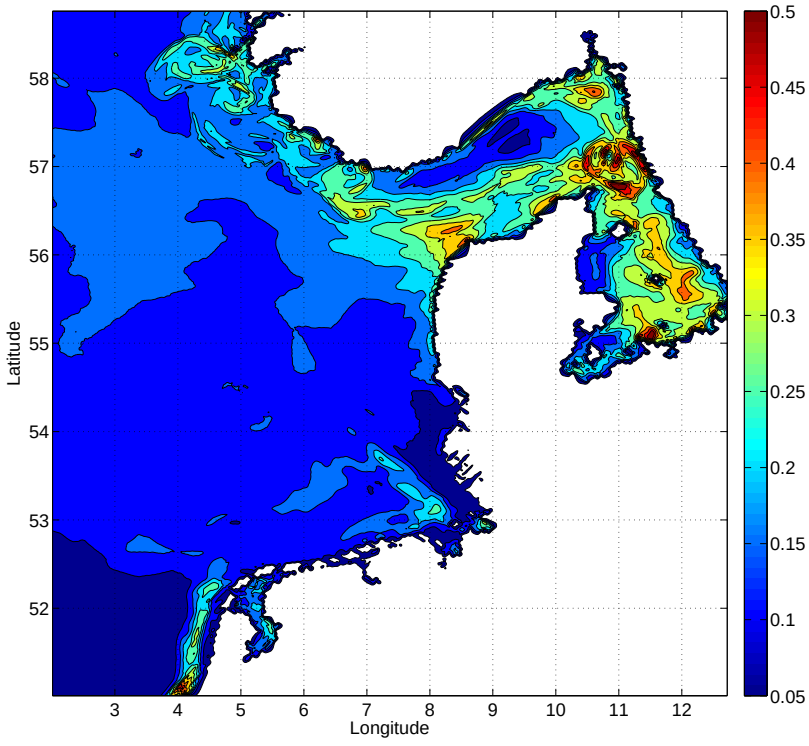

(b) Average ensemble standard deviation for 2m current speed (m/s) over the 60 hour period.

Figure 5.3: Average ensemble mean and average ensemble standard deviation for current speed. Areas with a large standard deviation is an indication of large ensemble spread for that area during the forecast period.

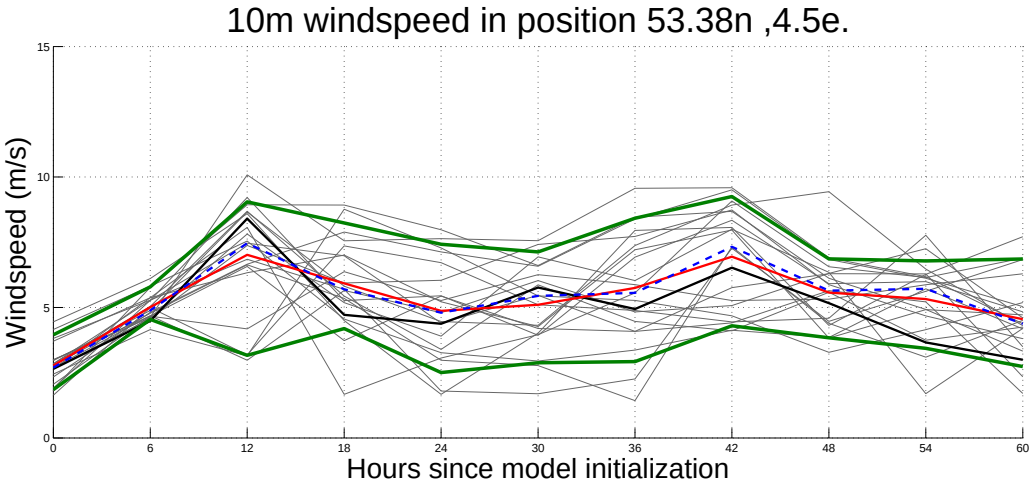

(a)

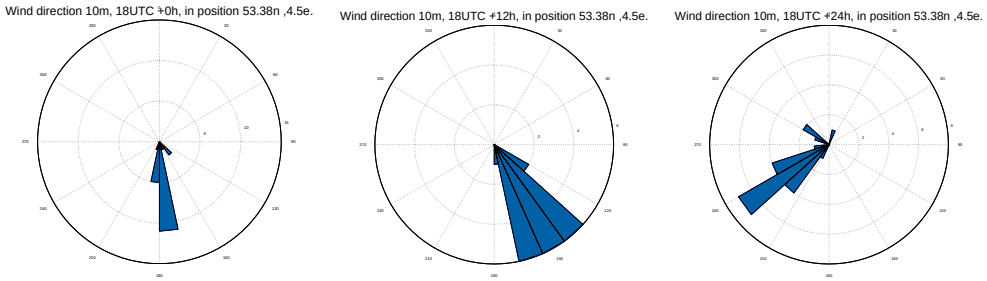

(b) +00h **(c)** +12h **(d)** +24h

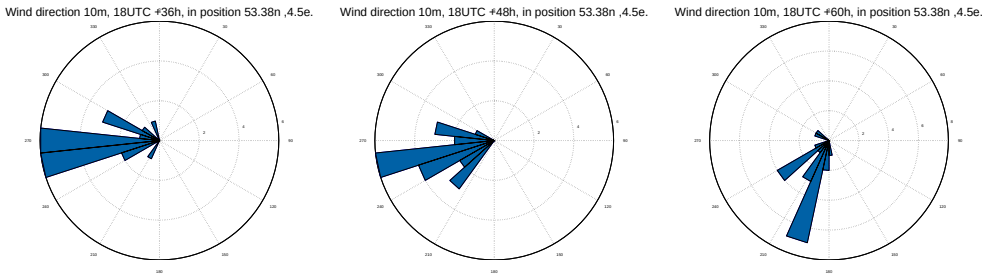

(e) +36h **(f)** +48h **(g)** +60h

Figure 5.4: Wind speed and direction for position 53.38 °N 004.50 °E (Station 1 in Figure 5.1). The thin grey lines in panel a) indicate each ensemble member, the black line is the control member, the bottom green line is the 10-percentile, the top green line is the 90-percentile, the dashed blue line is the median, and the red line is the average. The direction plots in panel b) - g) indicates the direction from which the wind is coming at the given lead time of the 18UTC forecast. The size of the blue area indicate the number of ensemble members within this sector (note that the axis are variable). There are 30 sectors (each sector is 12 °). North is up, east is to the right, south is down and west is to the left.

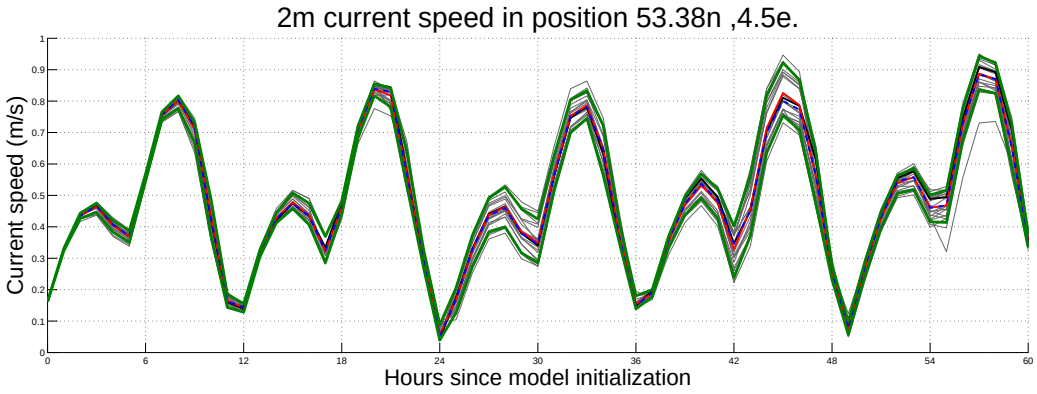

(a)

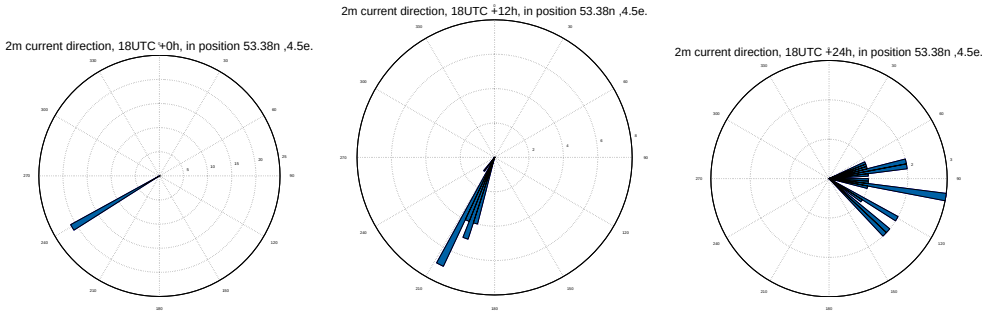

(b) +00h **(c)** +12h **(d)** +24h

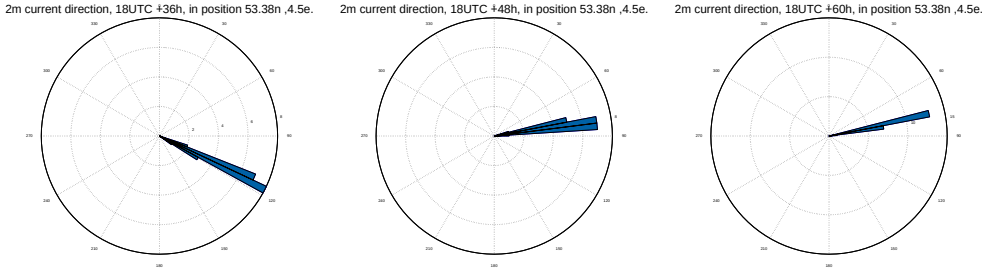

(e) +36h **(f)** +48h **(g)** +60h

Figure 5.5: Current speed and set direction for position 53.38 °N 004.50 °E (Station 1 in Figure 5.1). The thin grey lines in panel a) indicate each ensemble member, the black line is the control member, the bottom green line is the 10-percentile, the top green line is the 90-percentile, the dashed blue line is the median, and the red line is the average. The direction plots in panel b) - g) indicates the set direction (the direction the current flows) at the given lead time time of the 18UTC forecast. The size of the blue area indicate the number of ensemble members within this sector (note that the axis are variable). There are 100 sectors (each sector is 3.6 °). North is up, east is to the right, south is down and west is to the left. Note the low spread in current speed and direction compared to the high spread in the speed and direction of the wind in Figure 5.4. This is due to tidal forcing which is the main source of currents at this station. The slight spread in current direction is merely due to phase differences.

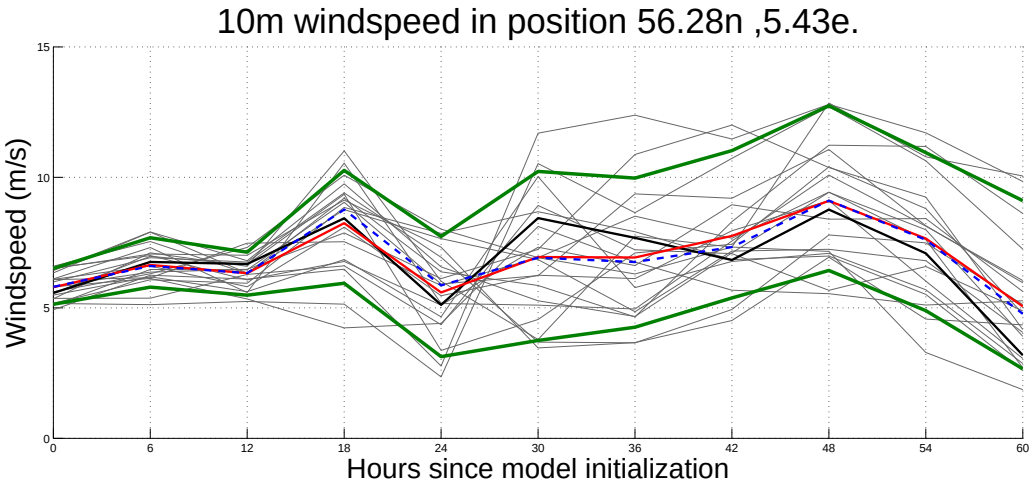

(a)

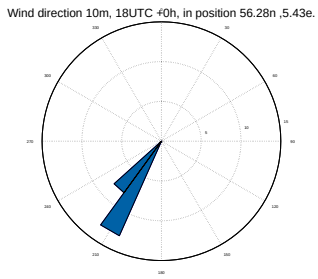

(b) +00h

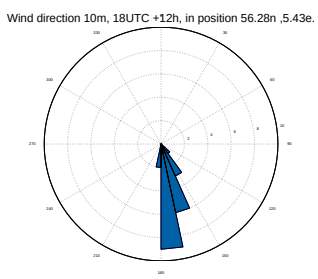

(c) +12h

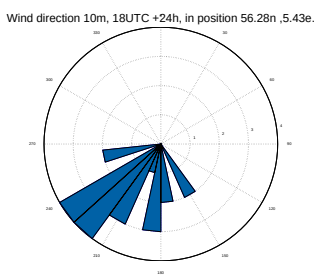

(d) +24h

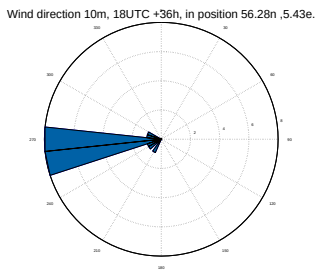

(e) +36h

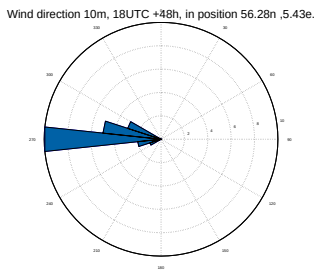

(f) +48h

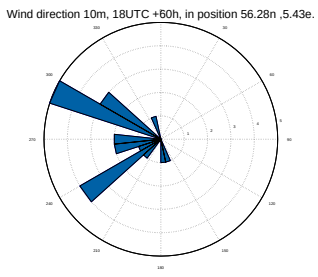

(g) +60h

Figure 5.6: As Figure 5.4, but for position 56.28 °N 005.43 °E (Station 2 in Figure 5.1). Note the spread in wind speed starting at +12h.

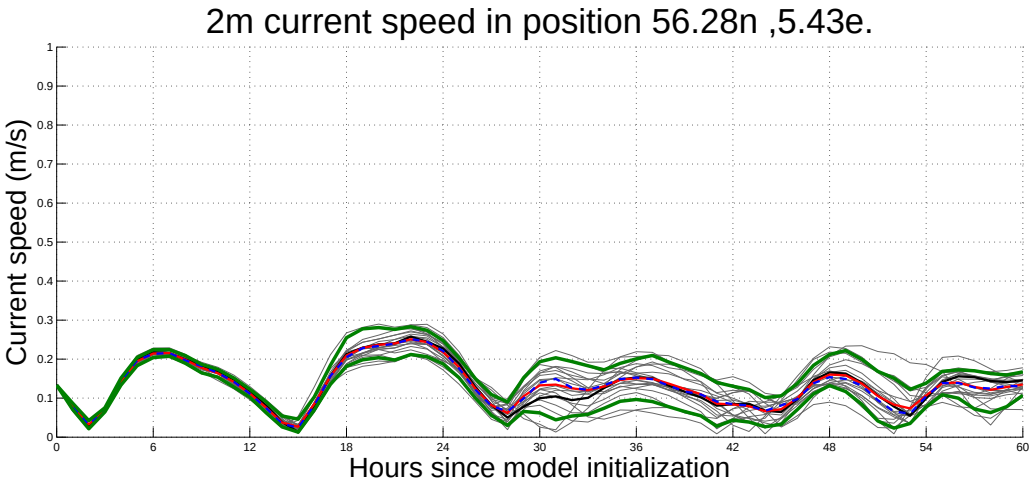

(a)

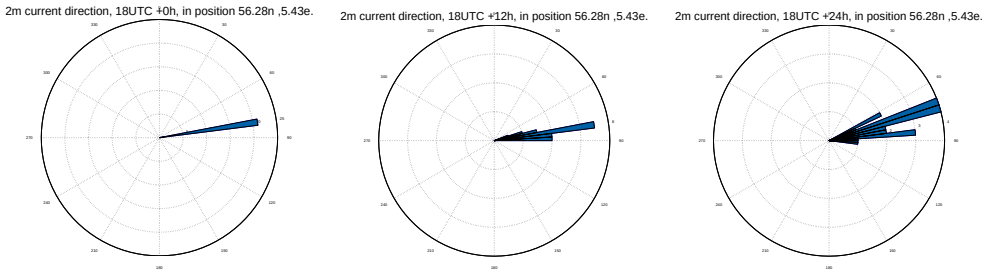

(b) +00h **(c)** +12h **(d)** +24h

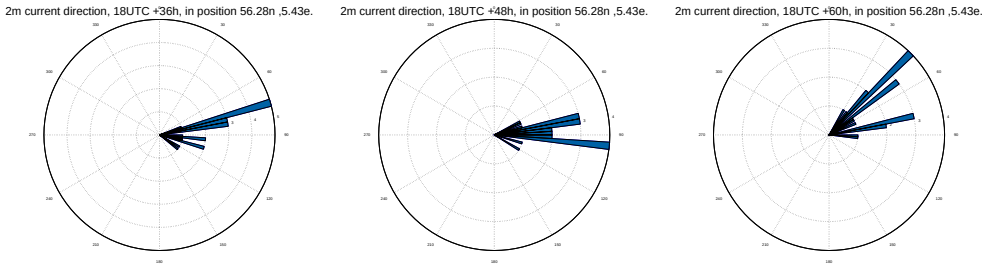

(e) +36h **(f)** +48h **(g)** +60h

Figure 5.7: As Figure 5.5, but for position 56.28 °N 005.43 °E (Station 2 in Figure 5.1). Note the spread in current speed starting at +18h induced by the spread in wind speed and direction in Figure 5.6.

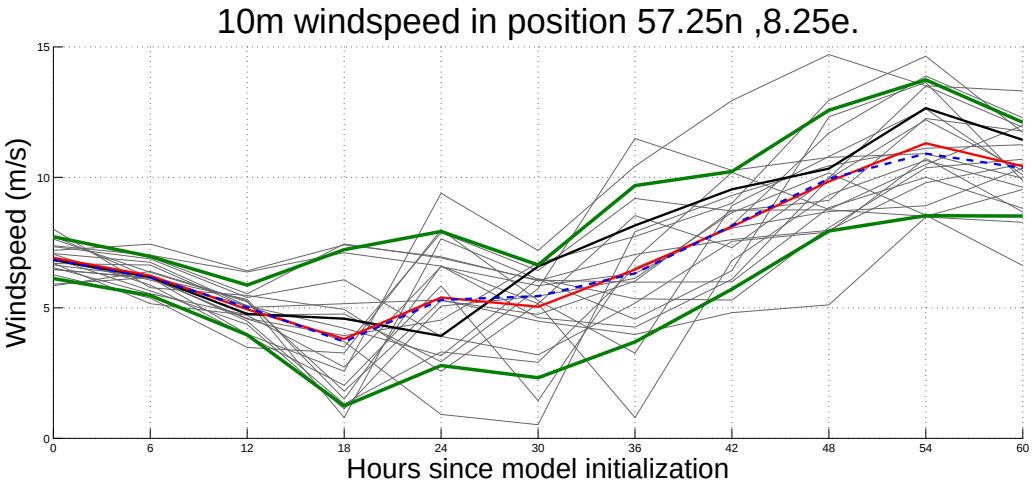

(a)

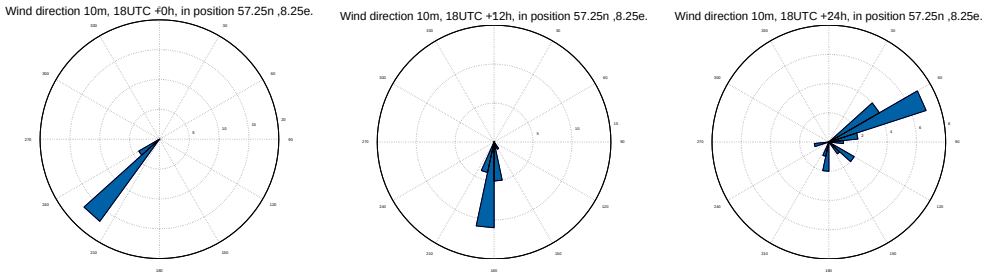

(b) +00h **(c)** +12h **(d)** +24h

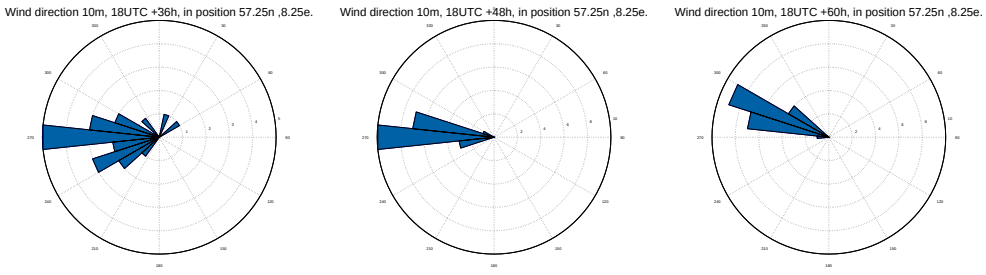

(e) +36h **(f)** +48h **(g)** +60h

Figure 5.8: As Figure 5.4, but for position 57.25 °N 008.25 °E (Station 3 in Figure 5.1). Note the spread in wind speed starting at +12h.

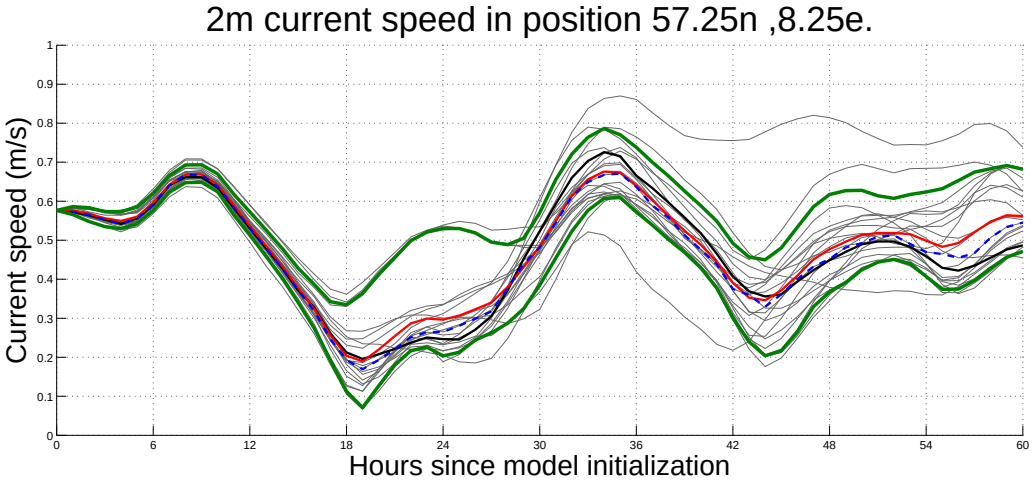

(a)

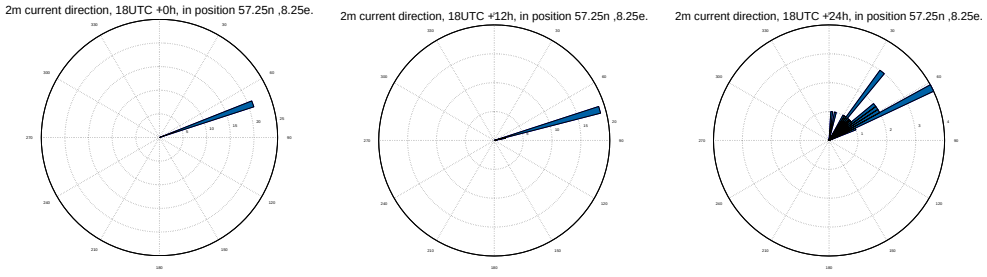

(b) +00h **(c)** +12h **(d)** +24h

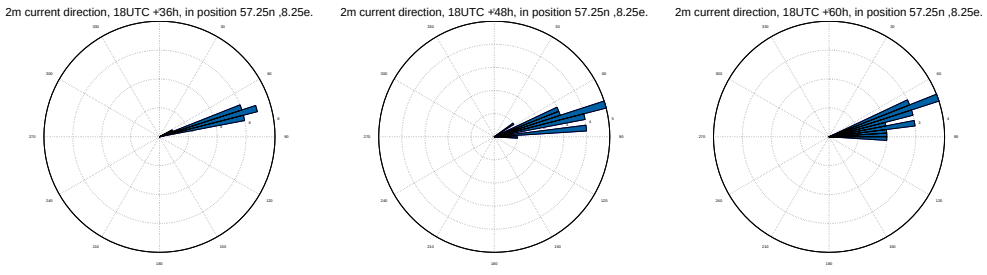

(e) +36h **(f)** +48h **(g)** +60h

Figure 5.9: As Figure 5.5, but for position 57.25 °N 008.25 °E (Station 3 in Figure 5.1). Note the spread in current speed from +18h induced by the difference in wind speed and direction in Figure 5.8. Also note that the direction of the current changes little during the 60 hours period. This is due to the station being placed within the Jutland Current.

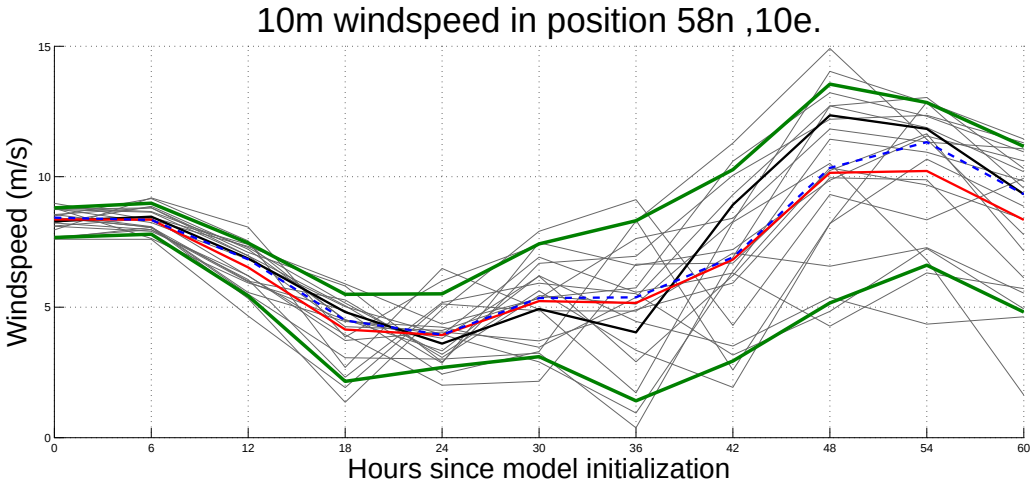

(a)

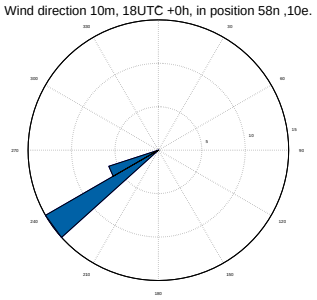

(b) +00h

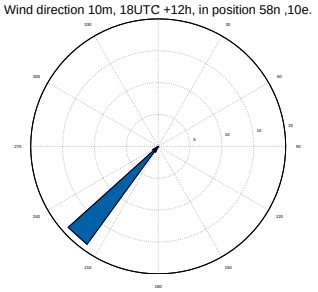

(c) +12h

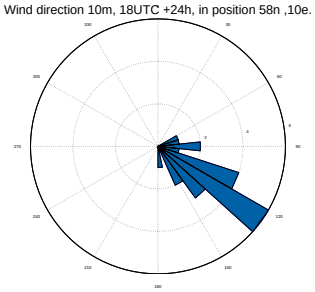

(d) +24h

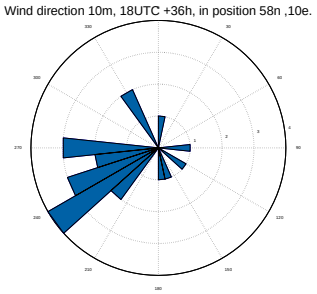

(e) +36h

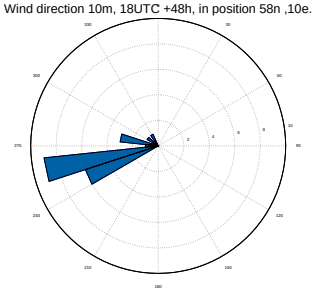

(f) +48h

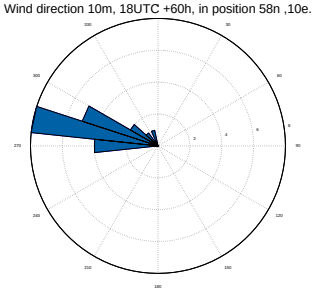

(g) +60h

Figure 5.10: As Figure 5.4, but for position 58.00 °N 010.00 °E (Station 4 in Figure 5.1). Note the spread in wind speed starting from +18h.

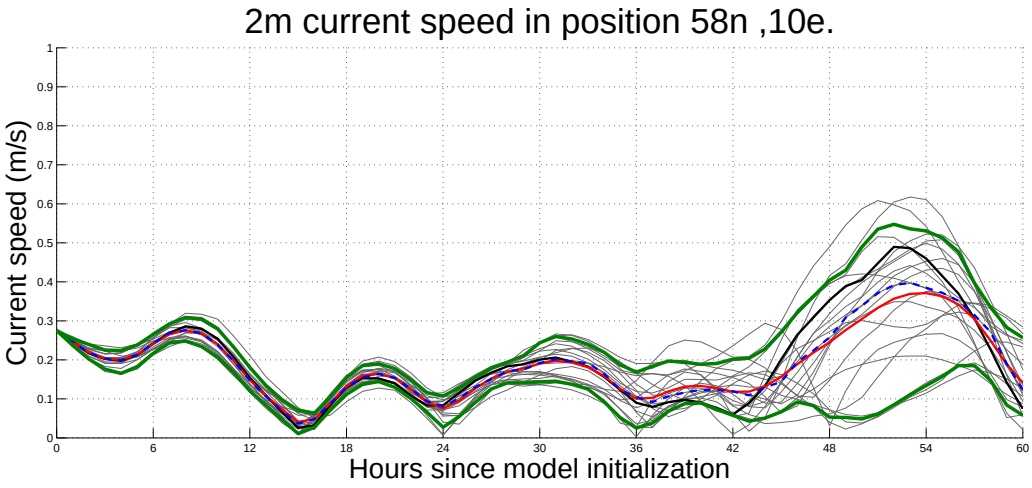

(a)

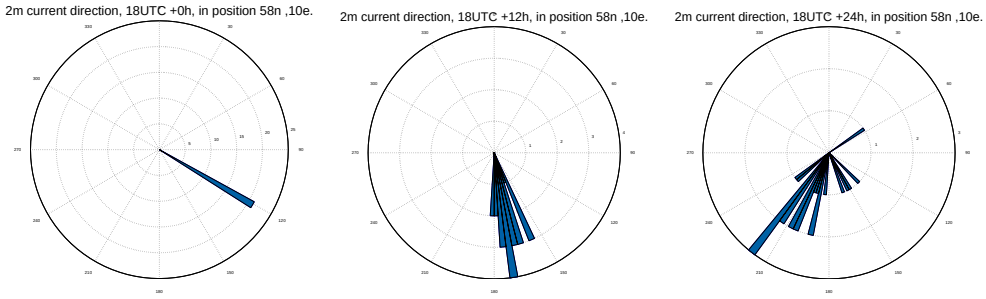

(b) +00h **(c)** +12h **(d)** +24h

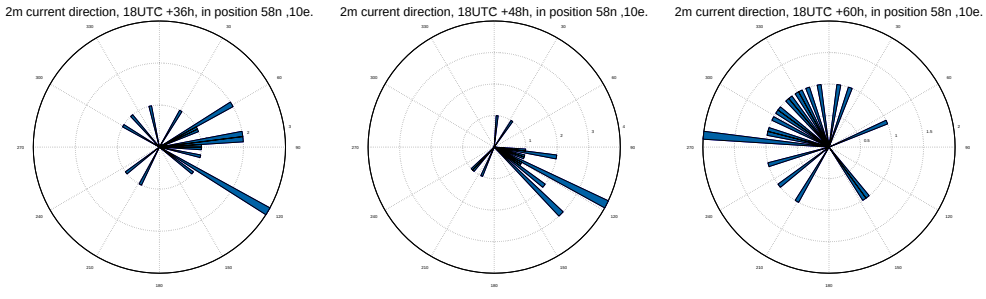

(e) +36h **(f)** +48h **(g)** +60h

Figure 5.11: As Figure 5.5, but for position 58.00 °N 010.00 °E (Station 4 in Figure 5.1). Note the large spread in current direction at +24h (panel d) and on. The largest spread in current speed occurs between +42h and +60h. This station is placed within the large eddy north of Skagen.

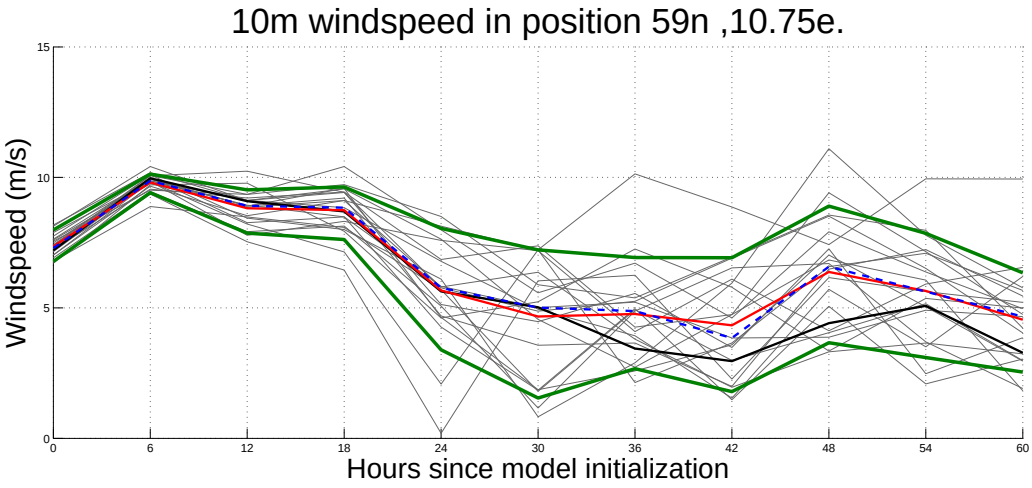

(a)

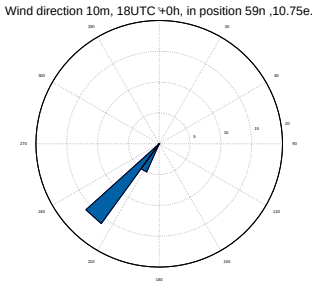

(b) +00h

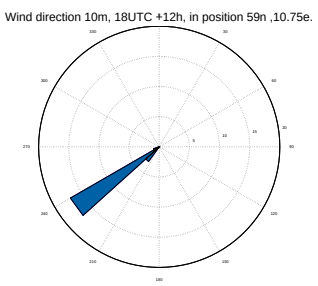

(c) +12h

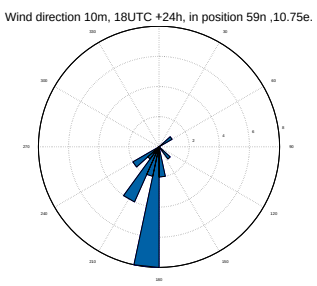

(d) +24h

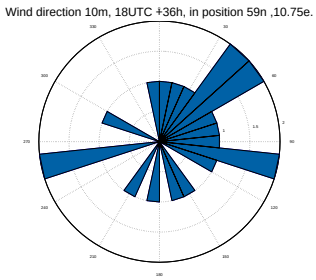

(e) +36h

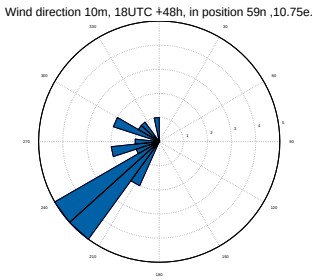

(f) +48h

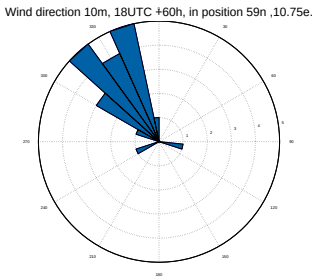

(g) +60h

Figure 5.12: As Figure 5.4, but for for position 59.00 °N 010.75 °E (Station 5 in Figure 5.1). Note the spread in wind speed from +18h.

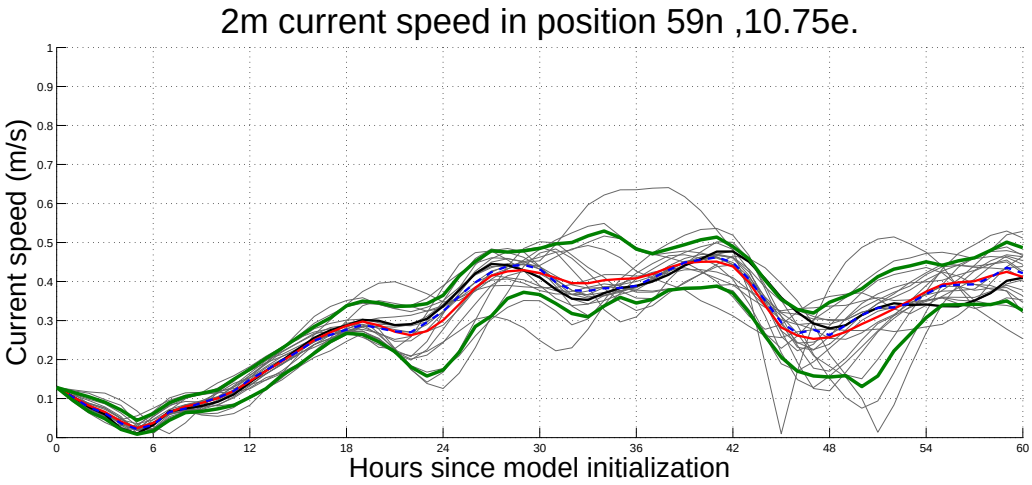

(a)

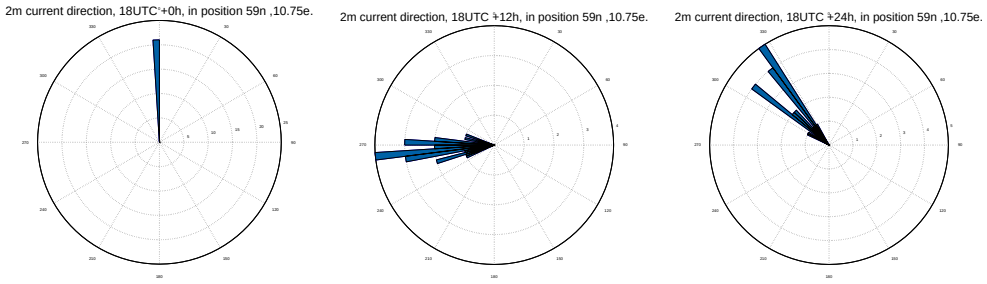

(b) +00h **(c)** +12h **(d)** +24h

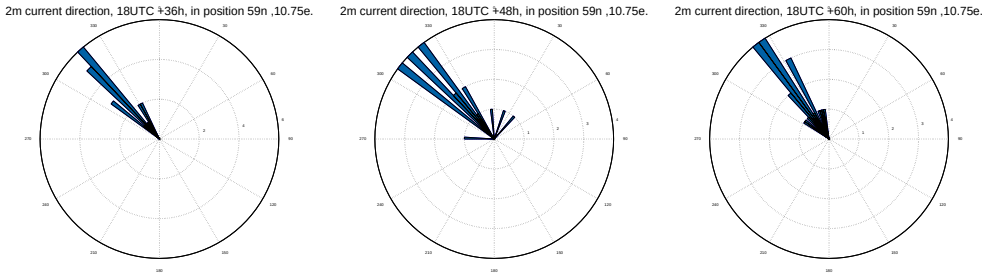

(e) +36h **(f)** +48h **(g)** +60h

Figure 5.13: As Figure 5.5, but for position 59.00 °N 010.75 °E (Station 5 in Figure 5.1). Note the spread in current speed from +18h. This is the same time as for the wind speed in Figure 5.12. This station is located close to the finish at Torbjørnskjær.

5.2 Deterministic experiments

5.2.1 Downwind case

Comparisons of the optimal routes calculated using the deterministic wind and current forecasts (the control member of LAMEPS and ROMS) as input (see Figure 5.14) gives the first indication of the effect of the current. Figure 5.14a shows the entire course, while Figure 5.14b gives a detailed picture of the routes as they enter Skagerrak.

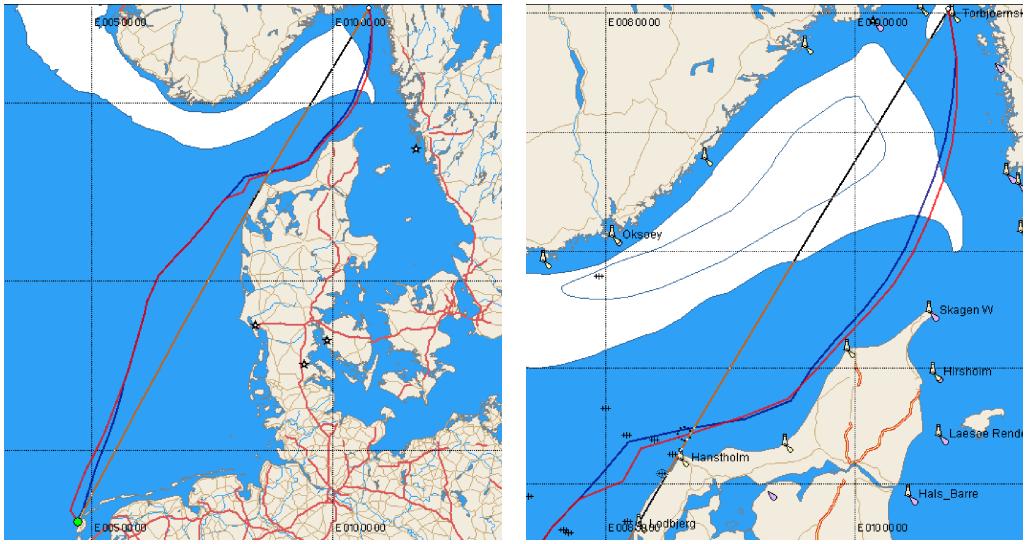

(a) **(b)**

Figure 5.14: Routes based on the control runs as input for the downwind case in a). Panel b) show the routes in Skagerrak. The blue line is the route based on wind input only (Experiment 1DN), while the red line is the route based on both wind and current input (Experiment 2DN). We observe that there are only minor differences between the two experiments.

We observe that the route based on both wind and current as input follows a slightly different path than the one using wind as input only. However, the difference is significant with regards to sailtime. The reason for the smal difference in location of the two routes is because the path of the optimal route using wind only (Experiment 1DN) goes through the areas of favourable currents. The most distinct features in Figure 5.14 is that the route which includes current as input (Experiment 2DN) head offshore in the beginning, follows closer to the west coast of Denmark at Hanstholm, and is a bit further east on the way north to the finish. This is to utilize the north-eastflowing Jutland Current which is more powerful closer to shore

at Hanstholm (see Figure 5.15 panel a), and the northflowing currents in the eastern part of Skagerrak (see Figure 5.15 panel b). These features can also be seen in Figure 4.2.

The sailtime along the optimal route that includes both wind and current as input (Experiment 2DN, the red line in Figure 5.14) is 46 hours and 21 minutes. If we choose to follow the route that was calculated using wind input only (Experiment 1DN, the blue line in Figure 5.14), the sailtime increases by 35 minutes when we include currents. This amounts to an increase of about 1.3% in the sailtime over the fastest route. It should be emphasized that a difference of 35 minutes in sailtime is significant with regards to winning or loosing a competition.

5.2.2 Upwind case

Figure 5.16 shows the routes calculated using the control runs for the upwind case. The addition of currents as input significantly modifies the paths of the optimal routes in this case. The largest difference is in Skagerrak, where the path of the optimal route using both wind and current as input (Experiment 2UP) follows very close to the Norwegian coast. This is due to the strong southflowing current along the southern coast of Norway, the Norwegian Coastal Current, which gives the sailboat a significant gain in speed.

The sailtime along the route calculated using both wind and current control forecast as input (Experiment 2UP, the red line in Figure 5.16 is 47 hours and 48 minutes. The sailtime along the route calculated using wind input only (Experiment 1UP, the blue line in Figure 5.16), if we include currents in the input is 48 hours and 28 minutes. This is a difference of 40 minutes, or an increase of 1.4% in the sailtime over the fastest route.

This is a prime example showing that the shortest route is not necessarily the fastest, and thus underscores the importance of including currents as input in the routing.

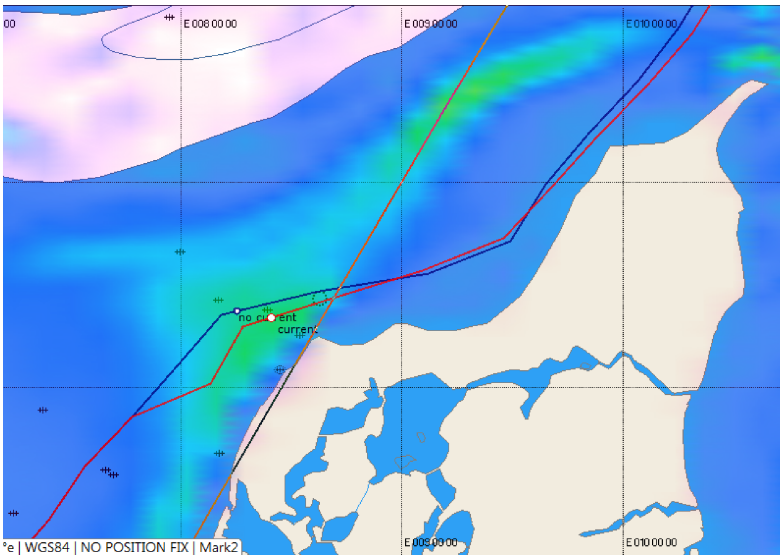

(a)

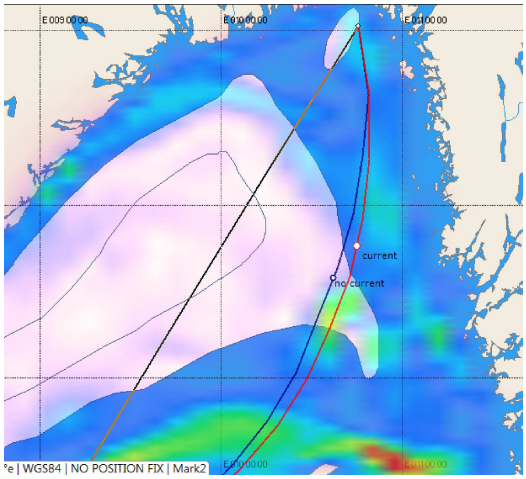

(b)

Figure 5.15: Currents along the route at 00UTC 22nd of May 2009 in panel a) and 12UTC 22nd of May 2009 in panel b). More intense color like green, yellow and red indicates areas of stronger currents. The same current patterns can be viewed in Figure 4.2.

(a)

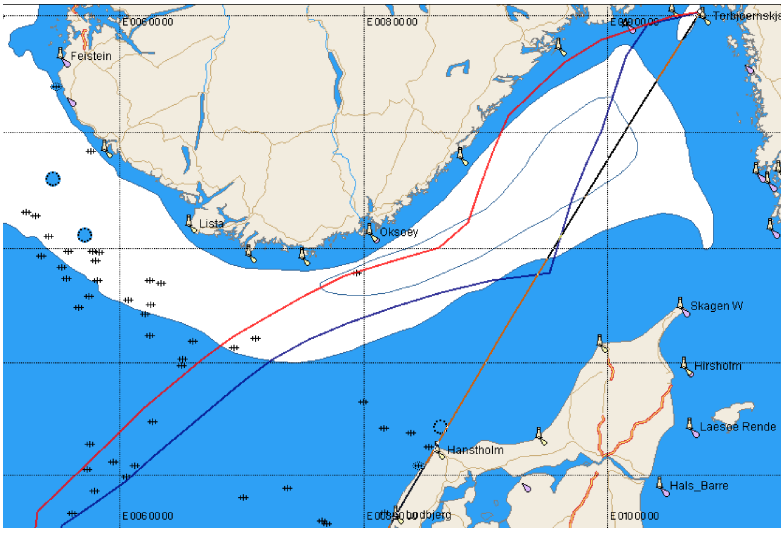

(b)

Figure 5.16: As Figure 5.14, but for the upwind case, i.e. Experiment 1UP (blue line) and 2UP (red line).

5.3 Probabilistic experiments

Using this approach we have to calculate an ensemble of routes. The generation of this ensemble is based on the 21 ensembles of wind and current input. There are 21 routes calculated for each of the Experiment 3 trough 6 described in Chapter 4.

5.3.1 Downwind case

The results for this case is derived through the four experiments 3DN, 4DN, 5DN and 6DN. The derived optimal routes for each of the experiments are displayed in Figure 5.17.

Figure 5.18 show the wind and current conditions the boat is subjected to as it follows along each of the optimal routes in Experiment 5DN. Note the spread in the ensembles as a function of how far along the route the boat has sailed. We observe that this spread increases as time increases in accordance with the lead time of the forecast. Note that after 15 integration steps (one integration step equals approximately 10 nautical miles), there is a considerable spread in wind speed in panel a), but it takes another 10 integration steps before we observe any significant spread in the wind direction in panel b), currents speed in panel c) and current direction in panel d).

We observe in Figure 5.17 that as we add currents to the input in the routing program, the geographical spread of the optimal routes change. To be able to quantify this change in spread to get a measure of the effects of current in the routing process, we have calculated the geographical standard distance of the waypoints that span each route. Since each route consists of an equal number of waypoints (in our case 44), we calculate the standard distance of all waypoints number 1, then number 2 and so on. The geographical standard distance is calculated as outlined in Section 2.1. It is a measure of how the routes are spread out on the chart. Lower standard distance indicate lower spread in the routes and vice versa. Figure 5.19 show the standard distance for the 21 routes of each of the three experiment 3DN to 5DN. Experiment 6DN was not analyzed because the spread in the routes is almost non existent.

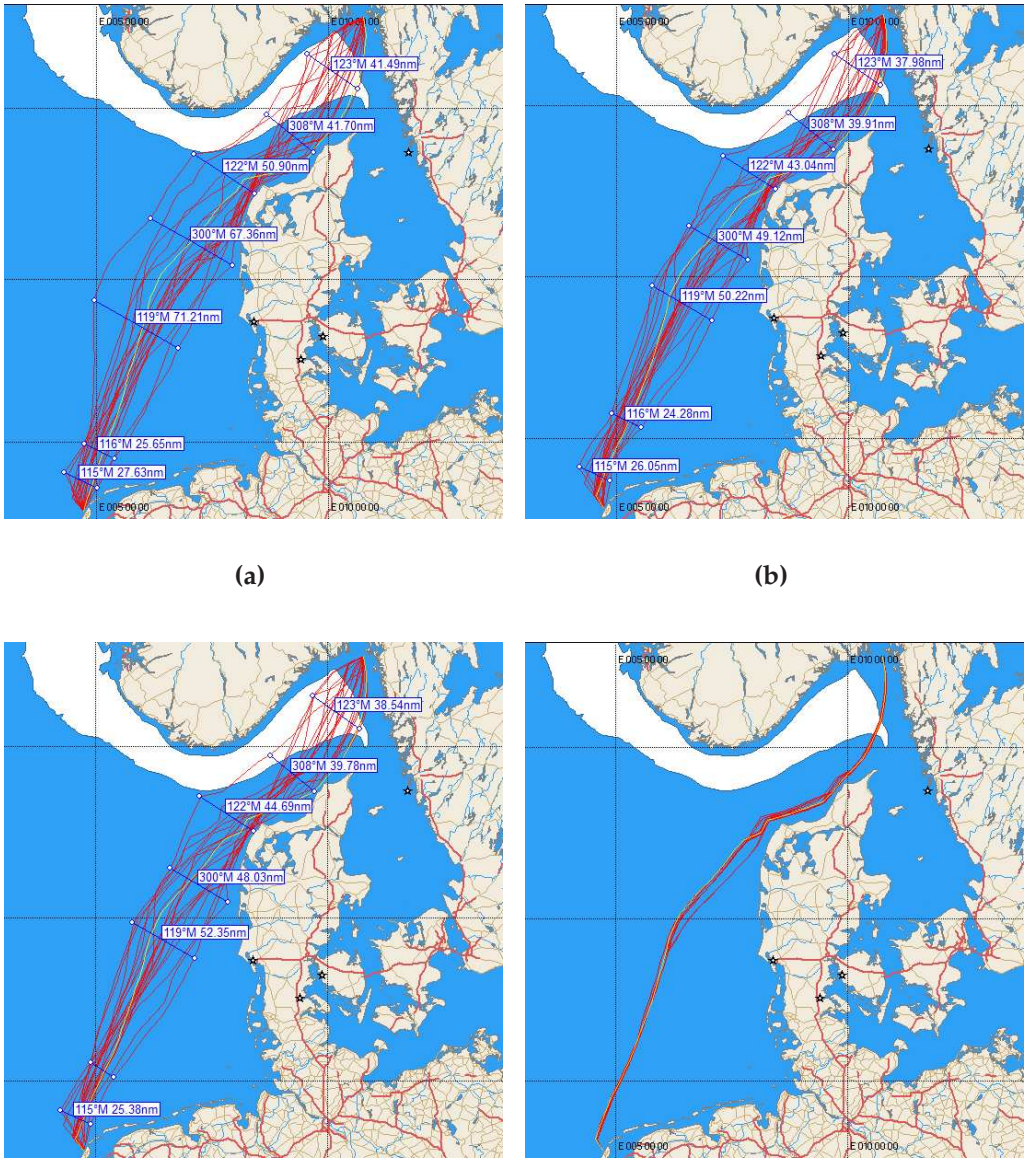

(a) **(b)**

(c) **(d)**

Figure 5.17: Optimal routes for the experiments in the downwind case. In a) Experiment 3DN, in b) Experiment 4DN, in c) Experiment 5DN and in d) Experiment 6DN. The blue lines across the routes and the number boxes indicate the distance across the ensemble of routes. The route given by the yellow line is the path suggested by the control member of the forecast ensemble.

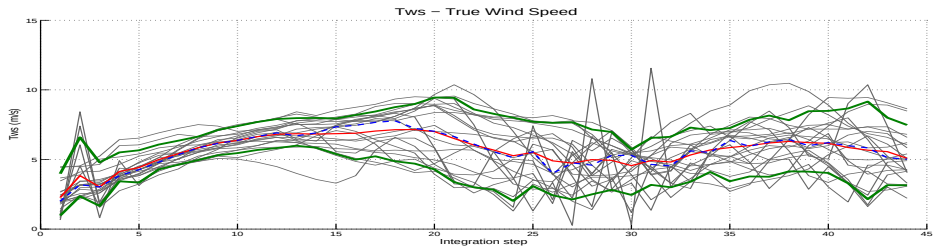

(a)

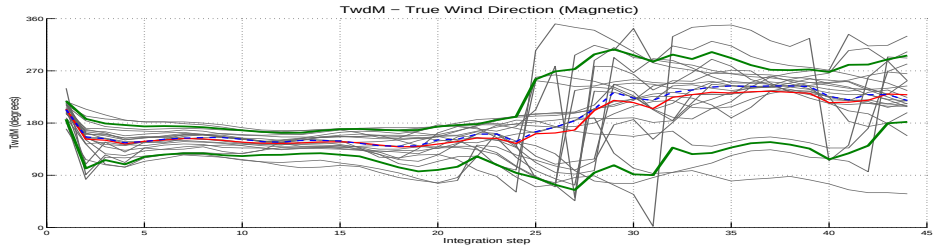

(b)

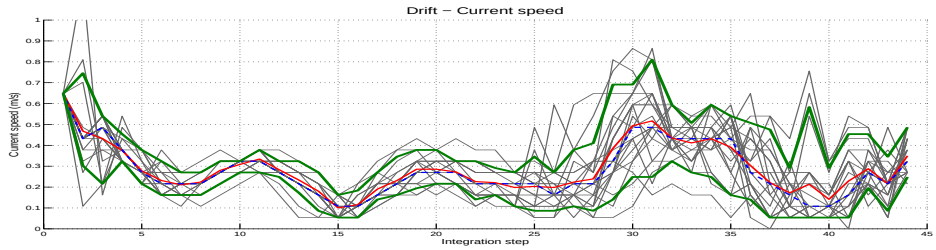

(c)

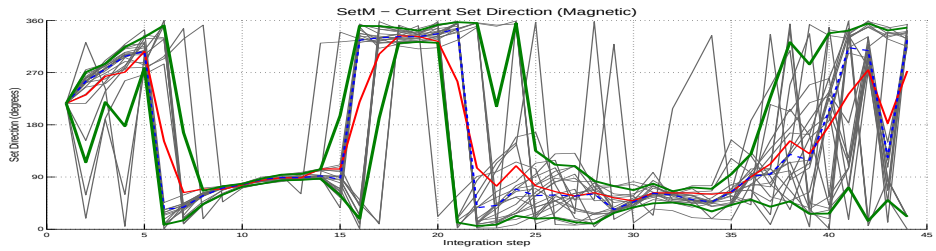

(d)

Figure 5.18: Graphs showing wind and current conditions the boat is subjected to as it sails along the optimal routes suggested by the experiment using both wind and current ensembles (Experiment 5DN). The grey lines indicate each ensemble member, the bottom green line is the 10-percentile, the top green line is the 90-percentile, the dashed blue line is the median, and the red line is the average.Panel a) is the wind speed, panel b) is the wind direction, panel c) is the current speed and panel d) is the current direction. Please note that as the wind direction in panel b) and current direction in panel d) passes trough north, it appears in the graph as an a abrupt jump.

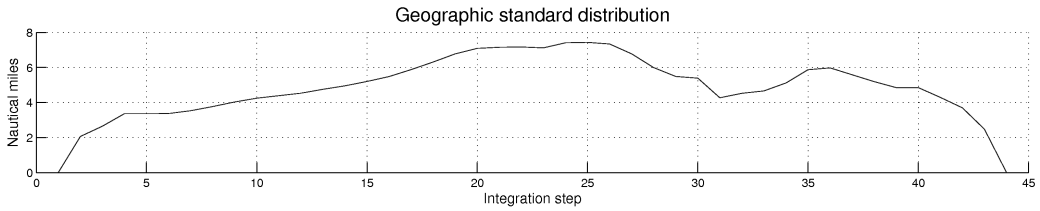

(a)

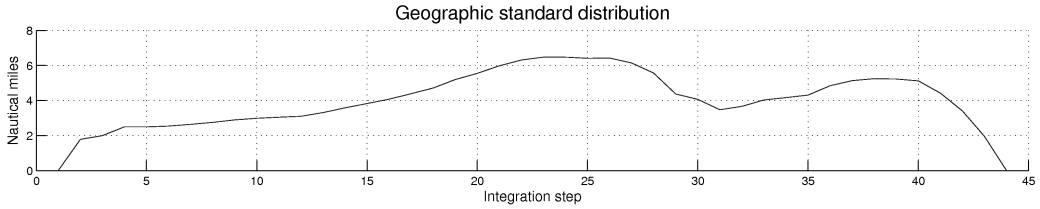

(b)

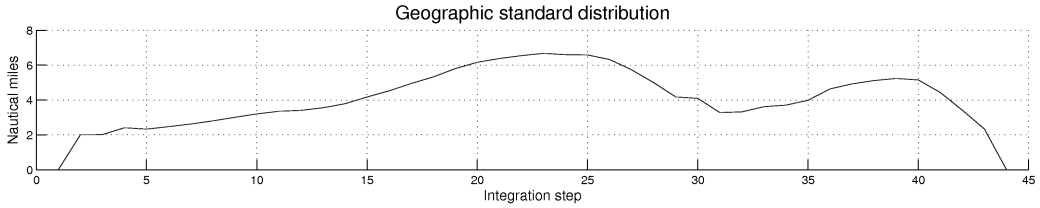

(c)

Figure 5.19: The geographical standard distance in nautical miles as a function of position along the optimal routes for the downwind case. This is a measure of how far apart from eachother the routes are. Experiment 3DN in a), Experiment 4DN in b) and Experiment 5DN in c).

Table 5.1 gives a summary of the statistics for sailtime and the route distance for each of the experiments in the downwind case. When we refer to the average sailtime and average route distance we refer to the arithmetic mean of the sailtimes and route distances of the ensemble of routes in each experiment. This is given by Equation 5.5, where $\overline{x}$ is the average of the ensemble of routes, N is the total number of routes (in our case 21) and x_i is the sailtime or route distance for route number i. The median sailtime and routes distance is found by arranging the sailtimes and route distances from lowest value to highest value and picking the one in the middle. The standard deviation, σ, for sailtime and route distance is found through Equation 5.6, where N is the total number of routes, x_i is the sailtime or route distance for route number i and $\overline{x}$ is the average of the ensemble of routes. The significance of the data presented in Table 5.1 will be discussed in Chapter 6.

$$\overline{x} = \frac{1}{N}\sum_{i=1}^{N} x_i \tag{5.5}$$

$$\sigma = \sqrt{\frac{1}{N}\sum_{i=1}^{N} (x_i - \overline{x})^2} \tag{5.6}$$

Experiment	**3DN**	**4DN**	**5DN**	**6DN**
Average sailtime	45h 47m	44h 56m	44h 55m	46h 26m
Median sailtime	45h 41m	44h 49m	44h 52m	46h 26m
Standard dev. sailtime	1h 58m	1h 58m	2h 3m	0h 5m
Average route distance	432.75nm	433.68nm	434.83nm	440.05nm
Median route distance	432.27nm	433.52nm	432.82nm	440.6nm
Standard dev. distance	7.53nm	6.98nm	7.74nm	1.54nm

Table 5.1: Average, median and standard deviations for sailtime and route distance for the downwind case. Experiment number is according to Table 4.1. See the text in Section 5.3.1 for a thorough explanation of the terms used in this table.

5.3.2 Upwind case

The optimal routes for each of the experiments in the upwind case are depicted in Figure 5.20, i.e. the four experiments 3UP, 4UP, 5UP and 6UP.

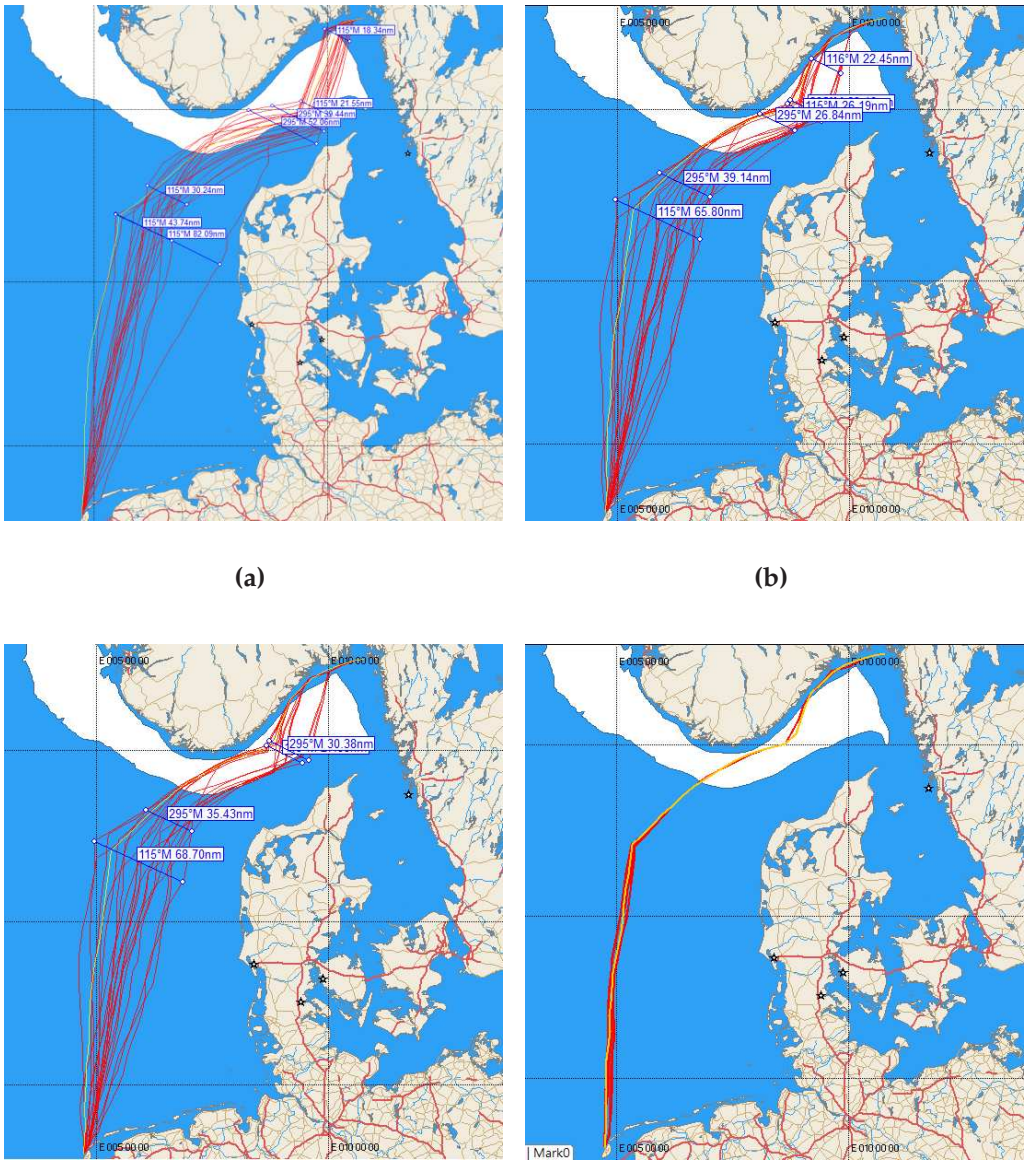

(a) **(b)**

(c) **(d)**

Figure 5.20: As Figure 5.17, but for the upwind case. In a) Experiment 3UP, in b) Experiment 4UP, in c) Experiment 5UP and in d) Experiment 6UP.

In Figure 5.21 we present the wind and current conditions the boat experiences as it follows each of the optimal routes in Experiment 5UP. This is the same figure as Figure 5.18, but for the upwind case. In this case we notice that the spread in wind speed in panel a) is quite consistent with the wind speed in the downwind case. However the wind direction is much more stable troughout the route. There is a trasition zone between integration step 15 and 25 where the wind shifts from south to west. An interesting note here is that while the wind in reality shifts trough north,

the routing program interprets it as a shift trough south because of the low time resolution of the GRIB-files (6 hours). The routing program does not look at the trends and interpret the data as a human could do, but simply shifts the wind linearly from one time-step to the other trough the smalles angle between them (Allsopp, 1998). The spread in current, both speed and direction, is similar to the downwind case.

The standard distance for the three experiments 3UP, 4UP and 5UP is shown in Figure 5.22.

Table 5.2 gives a summary of the statistics for sailtime and the route distance for each of the experiments in the upwind case. The averages and standard deviations is calculated using Equation 5.5 and 5.6. The contents of the table will be discussed in Chapter 6.

Experiment	**3UP**	**4UP**	**5UP**	**6UP**
Average sailtime	48h 21m	48h 11m	48h 10m	47h 47m
Median sailtime	47h 31m	47h 48m	47h 48m	47h 48m
Standard dev. sailtime	2h 47m	2h 24m	2h 26m	0h 4m
Average route distance	450.21nm	454.73nm	455.84nm	463.13nm
Median route distance	450.29nm	453.35nm	453.72nm	463.24nm
Standard dev. distance	5.82nm	10.21nm	9.61nm	0.73nm

Table 5.2: Same as Table 5.1, but for the upwind case. Experiment number is according to Table 4.1.

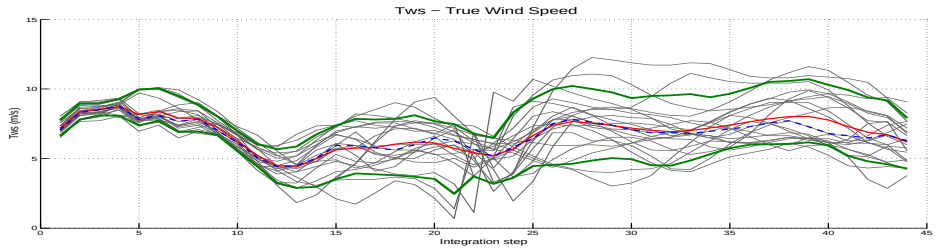

(a)

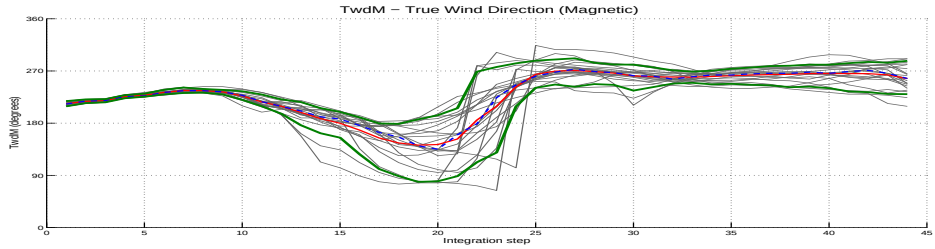

(b)

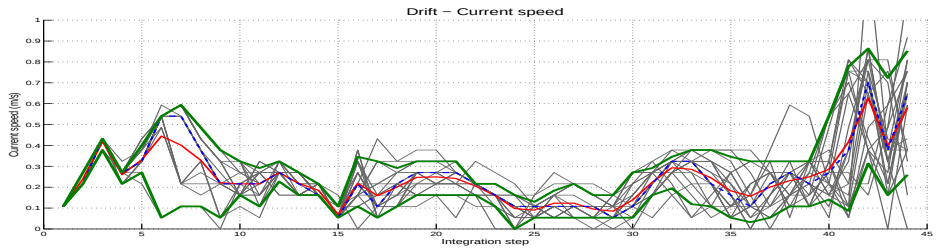

(c)

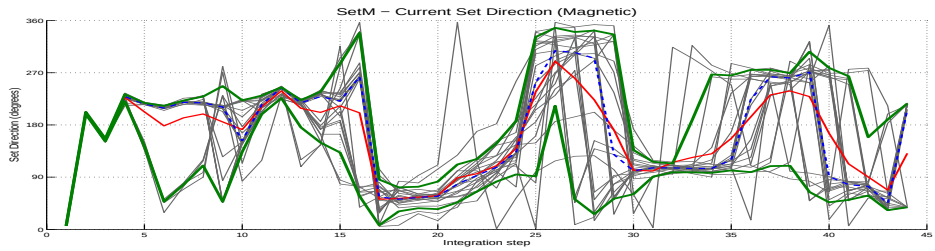

(d)

Figure 5.21: As Figure 5.18, but for Experiment 5UP.

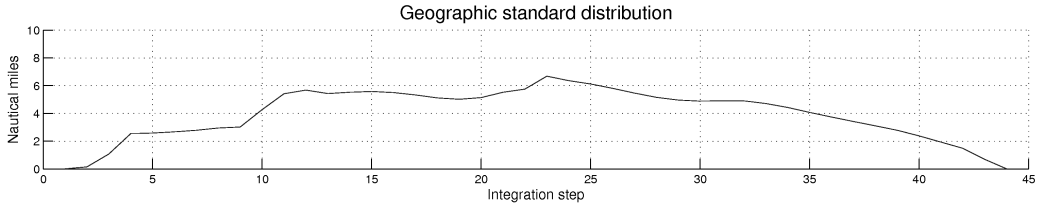

(a)

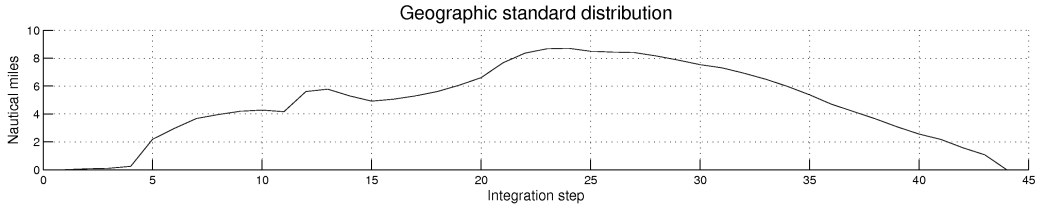

(b)

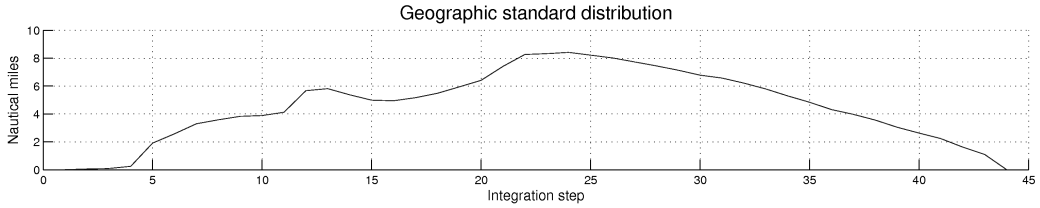

(c)

Figure 5.22: As Figure 5.19, but for the upwind case. Experiment 3UP in a), 4UP in b) and 5UP in c).

5.4 Averaged routes experiment

It is important to emphasize that, in this section, we do not use the routing capabilities of the routing program. The ensemble of 21 routes from each of the experiments 3DN, 4DN, 3UP and 4UP are averaged geographically according to Section 2.1, resulting in one new route, the average route, for each experiment. The main purpose of this is to assess if it is possible to develop a method for "minimum risk routing", instead of choosing a route based on one deterministic forecast only in weather situations associated with high forecast uncertainty. In these situations it is always valuable to have an ensemble of forecasts compared to a single deterministic one (Buizza, 2000). We need a method to determine which path is the least risky one to follow based on the ensemble of routes suggested by the routing program.

It is not possible to create a route that performs as good as, or better than, the optimal route for each ensemble member for all the ensemble members of the weather (and current) forecast. But it is possible to find routes that perform well under all the members of the weather (and current) ensemble. The method outlined in this section is merely about minimizing the risk, the possible loss (increase) in sailtime, when choosing one path over another when the weather forecast is uncertain.

In this section we refer to three different types of routes: The mean route, the median route and the control route. These three different types of routes was chosen to find the best approach to averaging the ensemble of routes.

- The "control route" is the suggested path to follow when using the deterministic forecasts as input to the routing program for each of the experiments 1DN, 2DN, 1UP and 2UP. The sailtime along this route acts as the benchmark for the two routes created trough the averaging techniques.
- The "mean route" was calculated using the *meanm*-function[1] (Mean location of geographic coordinates) in MATLAB. This was done by averaging the positions of waypoint number 1 for all of the 21 routes in the experiment in question into a mean waypoint number 1, the average of the positions of waypoint number 2 into mean waypoint number 2 and so on for all the 44 waypoints spanning the routes. When combined, this collection of mean waypoints spans what we call the mean route for that experiment.

[1] `http://www.mathworks.com/access/helpdesk/help/toolbox/map/ref/meanm.html`

- The "median route" was calculated simply by evaluating the longitude of the waypoints in each of the 21 routes in the experiment in question. Since the course is oriented mainly north-south, this method gives a satisfying result. This, of course, would not be the case for a route that deviates more from the north-south course axis, and the method would in that case need further development. The calcuation was done by picking all of waypoints number 1, sorting the waypoints according to increasing longitude, and picking the waypoint with the middle value as longitude as median waypoint number 1. The same was done for all waypoints from 2 to 44. The collection of median waypoints are, when combined, what we refer to as the median route.

The evaluation of the performance of these three different types of routes was done by feeding the mean, median and control routes for each experiment back into the routing program, and using the routing program to simply calculate the time it would take to follow each of the routes for each ensemble member input. This was done for each route for the weather and current input used in Experiment 3DN, 3UP, 4DN and 4UP. This gave us 21 possible sailtimes along each route in each experiment (one for each ensemble member). We then calculated the average (Equation 5.5), median and standard deviations (Equation 5.6) for for the sailtimes along the mean, median and control routes for each experiment. Put another way, this gives us the time it would take, on average, to follow the three different paths given that any random weather forecasts within the LAMEPS ensemble would occur.

5.4.1 Downwind case

Figure 5.23 show the mean, median and control routes using wind ensemble only (Experiment 3DN) in a) and wind ensemble with deterministic current (Experiment 4DN) in b) as input in the routing program for the downwind case. The statistics for the sailtime along the three different routes is shown in Table 5.3 and 5.4.

Route	**'Mean-3DN'**	**'Median-3DN'**	**'Control-3DN'**
Average sailtime	47h 28m	47h 29m	48h 41m
Median sailtime	47h 23m	47h 25m	48h 38m
Std.dev. sailtime	2h 20m	2h 24m	2h 17m

Table 5.3: Average and median sailtimes and standard deviations (std.dev.) for sailtimes for the averaged routes experiment for the downwind case for routes based on wind ensemble only, no current (Experiment 3DN).

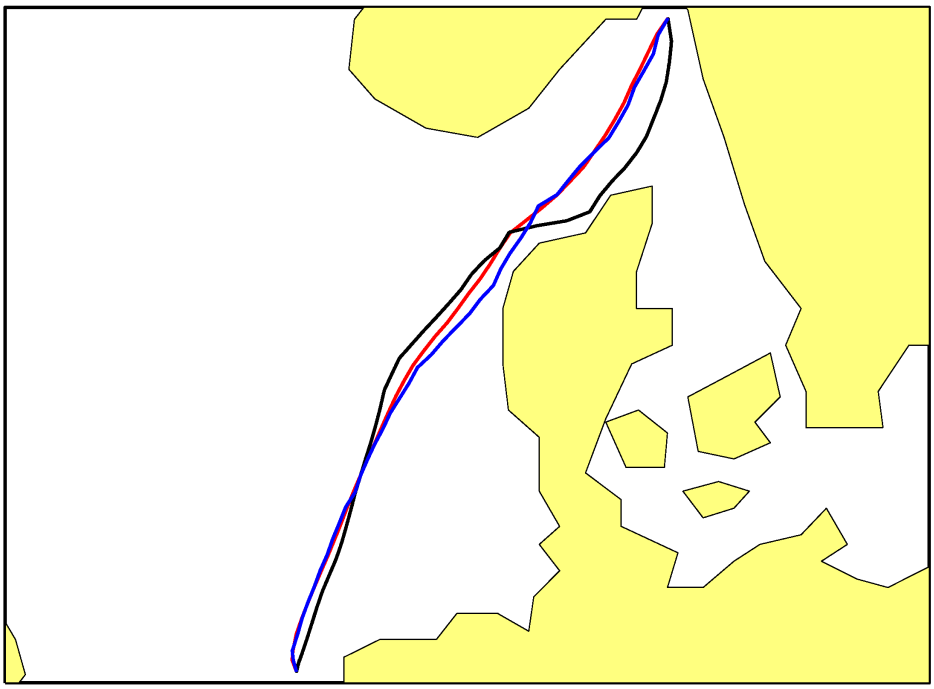

(a)

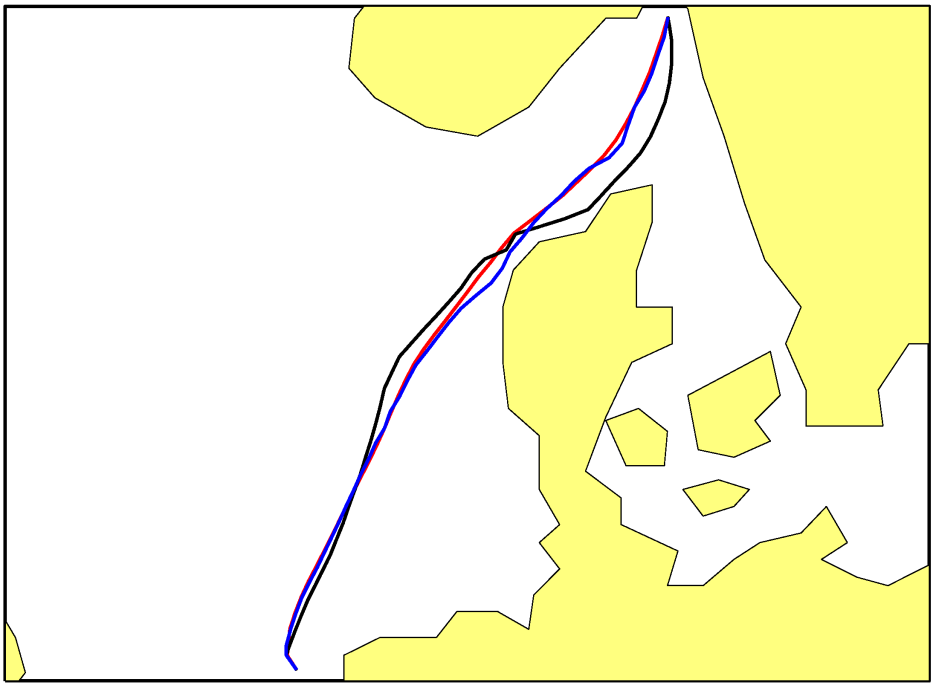

(b)

Figure 5.23: Averaged routes for the downwind case. In a) the routes based on Experiment 3DN and in b) the routes based on Experiment 4DN. The red line is the geographical mean route, the blue line is the geographical median route and the black line is the route based on the control member of the ensemble.

Route	'Mean-4DN'	'Median-4DN'	'Control-4DN'
Average sailtime	46h 45m	46h 48m	47h 39m
Median sailtime	46h 38m	46h 39m	47h 11m
Std.dev. sailtime	2h 30m	2h 35m	2h 17m

Table 5.4: As Table 5.3, but for the downwind case for averaged routes based on wind ensemble and deterministic current (Experiment 4DN).

5.4.2 Upwind case

Figure 5.24 show the mean, median and control routes using wind ensemble only (Experiment 3UP) in a) and wind ensemble with deterministic current (Experiment 4UP) in b) as input in the routing program for the upwind case. The statistics for the sailtime along the three different routes is shown in Table 5.5 and Table 5.6.

Route	'Mean-3UP'	'Median-3UP'	'Control-3UP'
Average sailtime	49h 38m	49h 53m	50h 10m
Median sailtime	48h 25m	48h 49m	49h 12m
Std.dev. sailtime	3h 25m	3h 23m	3h 46m

Table 5.5: As Table 5.3, but for the upwind case for averaged routes based on wind ensemble only, no current (Experiment 3UP).

Route	'Mean-4UP'	'Median-4UP'	'Control-4UP'
Average sailtime	50h 10m	50h 20m	49h 59m
Median sailtime	49h 53m	49h 34m	48h 24m
Std.dev. sailtime	3h 24m	2h 05m	3h 54m

Table 5.6: As Table 5.3, but for the upwind case for averaged routes based on wind ensemble and deterministic current (Experiment 4UP).

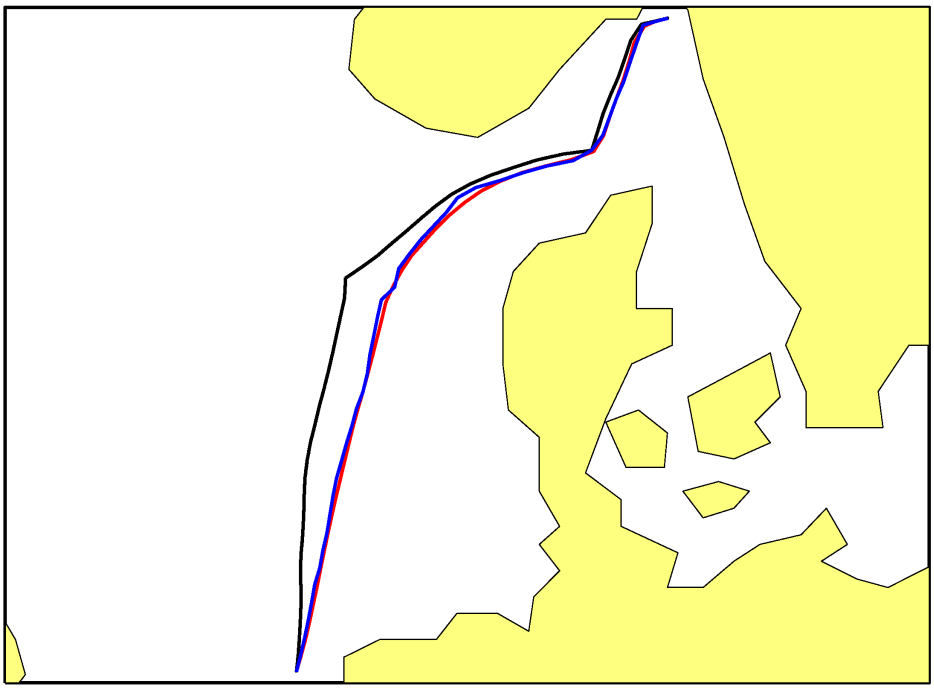

(a)

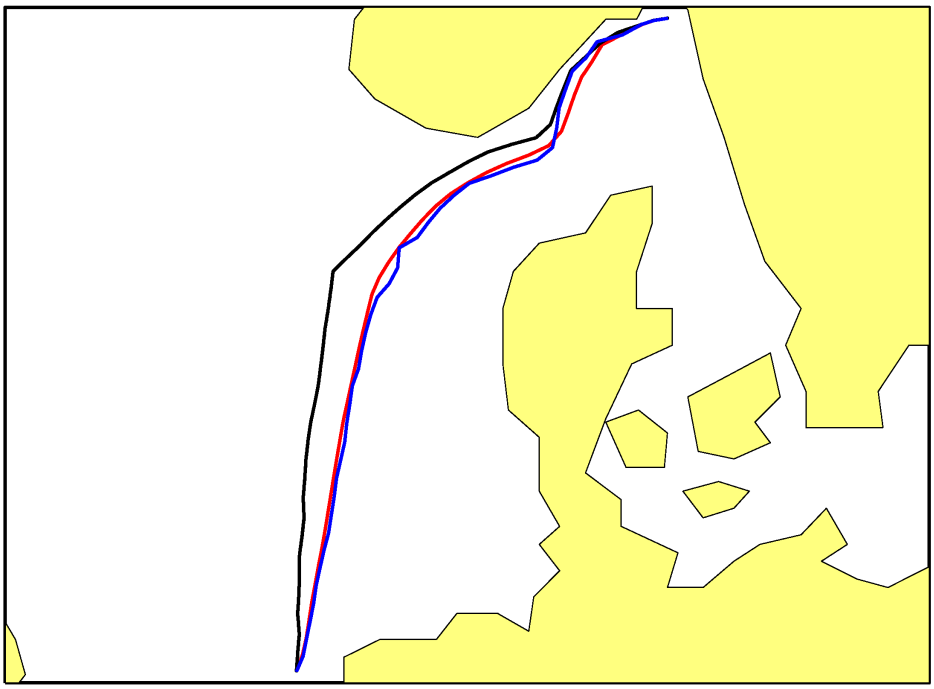

(b)

Figure 5.24: As Figure 5.23, but for the upwind case. In a) the routes based on Experiment 3UP and in b) the routes based on Experiment 4UP.

Chapter 6

Discussion

In earlier work on the subject of weather routing for sailboats (e.g., Allsopp, 1998, page 61) it is claimed that the current can be predicted with much greater accuracy than the wind, and that the need for ensemble forecasting for the ocean is not as useful as for the atmosphere. We both agree and disagree with this statement. We partly agree that the need for an ensemble for the ocean is not as great as for the atmosphere, but disagree with the statement that the current is much more predictable than the wind. As we show in Figure 5.3(b), there is a significant standard deviation for the current speed among the ensemble members in certain areas. This indicates that there are regions that are more sensitive than others to varying wind forcing. This spread can also be seen in figures 5.4 through 5.13. In the 60 hour period studied in this thesis, the most sensitive areas are in Skagerrak and Kattegat (east of 8 °E). As mentioned earlier, areas with little or no standard deviation in the current ensemble are likely to have currents dominated by tides. It is quite obvious that in those regions, the need for ensemble forecasting of ocean currents is very limited, whereas in the areas influenced by wind forcing, such an ensemble provides valuable information about the current forecast uncertainty.

To answer the key question regarding the importance of currents when the weather forecast is uncertain, we have used three different factors to study:

1. Visual inspection of the optimal routes.
2. The standard distance of the optimal routes (i.e. the geographical distribution).
3. Average and median sailtime, and the standard deviation for the sailtime.

We feel that these factors gives a good indication whether our hypothesis is supported or falsified.

The standard distance for the routes show how far apart from each other they are, and this quantifies the spread in the ensembles of routes. We observe in the plots for the downwind case (Figure 6.1, panel a and panel b) that the routes which includes currents (Experiment 4DN and 5DN), on average, has a standard distance of approximately 1 nautical mile less than those without currents (Experiment 3DN). Panel a in this figure represent the difference in standard distance between Experiment 3DN and 5DN. Positive values indicate that there is less spread in the experiment that includes current (5DN) than the one without (3DN). Panel b show the same as in panel a, but for Experiment 3DN and 4DN. Since the standard distance for the routes based on wind only in Figure 5.19a most of the time varies between 3.5 and 7 nautical miles, a 1 nautical mile reduction in the standard distance is quite significant. This general narrowing in the spread of the routes can also be seen in Figure 5.17.

In the upwind case the spread is a bit different than in the downwind case. The overall spread in the routes for the upwind case is slightly larger for the two experiments including currents (Experiment 4UP and 5UP) than the one without (Experiment 3UP). This is perhaps best visualized by comparing the standard distance in Experiment 3UP to the two other experiments. This is done in Figure 6.2a and Figure 6.2b (positive values indicates less spread in the experiments including currents than the one without) and by visually inspecting the routes in Figure 5.20. In the two experiments including currents (Experiment 4UP and 5UP) there seems to be two different "regimes" (Figure 5.20b and c), one where the routes follow the Norwegian coast to take advantage of the southward Norwegian coastal current, and one where the routes go further offshore. This entails that for those ensemble members that gives a route that follows the coast, the current plays a major role in determining the routes. While for the remainder ensemble members this appears not to be the case.

To visualize the difference in standard distance between the experiments using the entire ensemble of current forecasts (Experiment 5DN and 5UP) and those using the deterministic current forecast only (Experiment 4DN and 4UP), we include a plot of the differences between 5DN and 4DN in Figure 6.1c, and between 5UP and 4UP in Figure 6.2c. Positive values indicate larger spread in the routes that make use of the ensemble of currents, than in those including the deterministic forecast only. As we discover in the two figures, the differences between the experiments are small. The largest difference is approximately 0.6 nautical miles for the downwind case and 0.75 nautical miles for the upwind case.

We also notice that in the upwind case there is less spread in the wind direction when sailing along the optimal routes (Figure 5.21b) than in the downwind case (Figure 5.18b). This low spread in wind direction in the upwind case is a major contributor to the fact that the routes in the up-

wind case are all very similar, and looks like they are merely shifted to the east and west of each other. This is in sharp contrast to the downwind case where the routes looks like they are ramdomly distributed over the race course. In the upwind case, the division into two regimes in the first third of the course, and the matter of fact that the change in wind direction occurs at slightly different times in the ensemble members, as seen in Figure 5.21b, is what generates the spread in the last two thirds of the course. In this part they enter the region of very predictable currents. As the wind turns from southerly to west, the fastest routes in the last half of the course are simply the straight lines to the finish as seen in Figure 5.20. As pointed out in Section 5.3.2, this change in wind direction is not very well resolved in the routing program due to low temporal resolution in the weather data. When the wind in reality changes anticlockwise from south to west over the 6 hours between the timesteps in the wind GRIB-file, the routing program interprets this change as a clockwise change in direction. This, as we point out later in Section 6.3, has a big impact on the performance of the average routes.

6.1 The ocean ensemble

As we mentioned earlier in Chapter 3, there is probably a large weakness in the way we have constructed our ocean ensemble. Because all the ensemble members, with different atmospheric forcing, was initiated from the same initial conditions (ICs), the ocean ensemble is most probably biased. This suspected bias is due to the fact that the ocean has a longer response time due to inertia than the atmosphere, and in takes more time for changes in the atmospheric forcing to produce changes in the ocean circulation. We have not done any validation of the ensemble, so we can not confirm this suspicion. Ideally, we should have had perturbed ICs for the ocean in the same way as for the atmosphere.

In our two cases, the upwind case and the downwind case, the difference between the routes based on the current ensemble and those based on the deterministic current forecast, does not differ significantly in either sailtime (Table 5.1 and Table 5.2) or in the geographical distribution (Figure 6.1c and Figure 6.2c). In the comparison of sailtimes we observe that the differences between the average sailtimes for the two experiments is 1 minute. For the medians for sailtime the difference is 3 minutes for the downwind case, and 0 minutes for the upwind case. The standard deviations for sailtime differs with a maximum of 5 minutes. All of these differences are negligible. When comparing route distances we see the same, that the differences between the experiments using the current ensemble (Experiment 5DN and 5UP) and the experiments using the deterministic

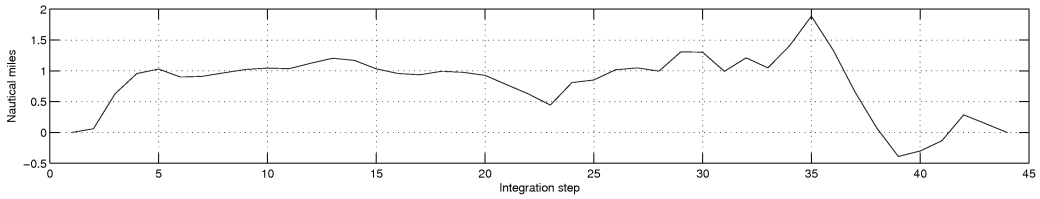

(a)

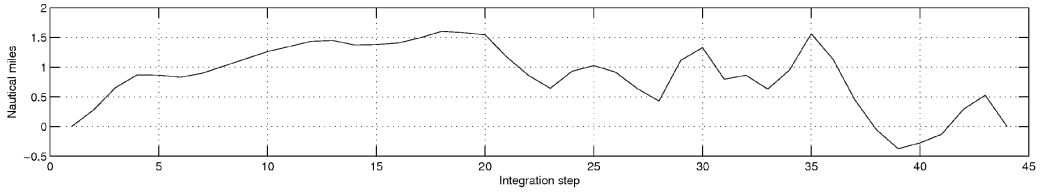

(b)

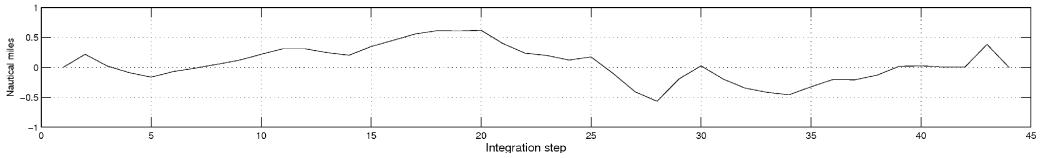

(c)

Figure 6.1: Differences in geographical standard distributions in nautical miles for the upwind case. In a) the difference between the optimal routes based on wind only (Experiment 3DN) and those based on the wind and current ensembles (Experiment 5DN). Positive values indicate larger spread in 3DN than in 5DN. In b) the difference between the optimal routes based on wind only (Experiment 3DN) and those based on wind ensemble and deterministic current (Experiment 4DN). Positive values indicate larger spread in 3DN than in 4DN. In c) the difference between the optimal routes based on the ensemble of currents (Experiment 5DN) and those based on the deterministic current (Experiment 4DN). Positive values indicate larger spread in the routes based on the current ensemble than in those based on the deterministic current.

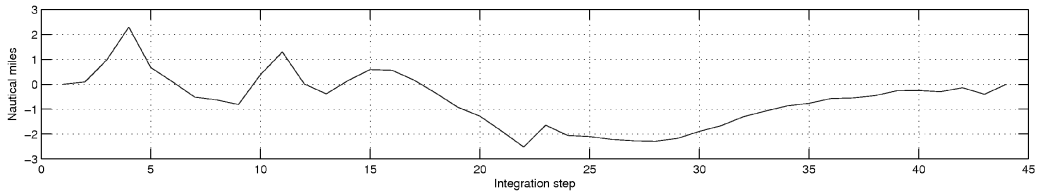

(a)

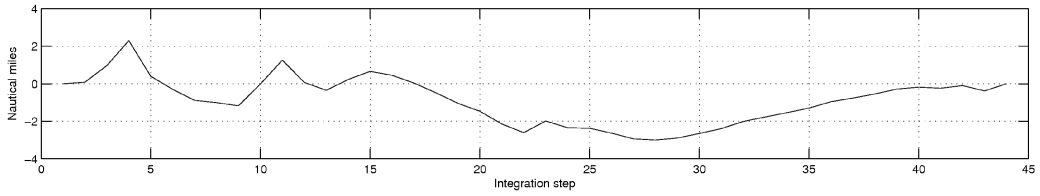

(b)

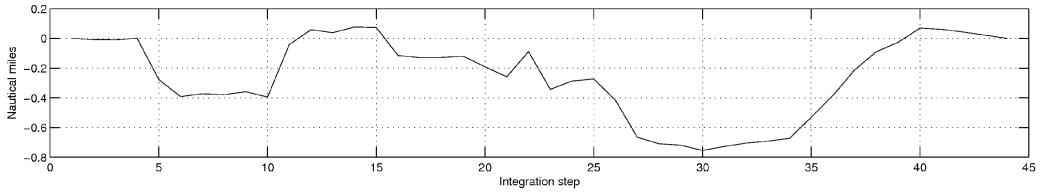

(c)

Figure 6.2: As Figure 6.1, but for the upwind case. In a) the difference between the optimal routes based on wind only (Experiment 3UP) and those based on the wind and current ensembles (Experiment 5UP). Positive values indicate larger spread in 3UP than in 5UP. In b) the difference between the optimal routes based on wind only (Experiment 3UP) and those based on wind ensemble and deterministic current (Experiment 4UP). Positive values indicate larger spread in 3UP than in 4UP. In c) the difference between the optimal routes based on the ensemble of currents (Experiment 5UP) and those based on the deterministic current (Experiment 4UP). Positive values indicate larger spread in the routes based on the current ensemble than in those based on the deterministic current.

current (Experiment 4DN and 4UP) are negligible. The same insignificant differences can be seen by visually inspecting the optimal routes in Figure 5.17 and Figure 5.20. Small differences in the current ensemble are not likely to result in any major differences in the optimal routes when the wind is kept the same (see Figure 5.20d and Figure 5.20d). This indicates that, although useful in some regions, the need for an ocean current ensemble in this case is superfluous. However, a figure like the one displayed in Figure 5.3b gives the user a better appreciation of how accurate the current forecast is, and identifies where there are areas of uncertainty.

The findings in Figure 5.3b corresponds well with the findings made by Albretsen and Røed (2010). The data presented here covers only a 60 hour time period, while the data presented by Albretsen and Røed (2010) cover 27 years. Nevertheless we still find many of the same main features and coastal currents. Thus the ocean current patterns for the chosen period are not deviating much from the average pattern (Albretsen and Røed, 2010; Røed and Fossum, 2004). A distinct difference is that within our period there are a few large eddies off the southern tip of Norway. These eddies are however robust features (e.g., Melsom, 2005) and are shown by Røed and Fossum (2004) and later by Fossum (2006) to be a recurrent feature. However in the average circulation pattern taken over several years the mesoscale features such as eddies are averaged out.

6.2 Limitations and suggested improvements

The LAMEPS atmospheric data has a 12km horizontal resolution. This should be sufficient to resolve differences in wind offshore, but for sailing close to the shore, higher resolution is desirable. The temporal resolution is only 6 hours. That is not enough to fully utilize the possible benefits of ensemble weather routing, or really weather routing at all. This is because the routing program does a linear interpolation of the weather data in time between the time-steps in the GRIB-files, and therefore loose valuable information about when sudden changes in the wind speed and direction occurs. Sudden changes that can happen in order of a few minutes, get averaged, and will in the routing happen over a timescale of 6 hours (between steps in the model). Also, the routing program does not know if the wind shifts clockwise or anti-clockwise when the change in direction from one time-step to another is large.

Another important limitation is the optimal routing resolution in the routing program. This resolution should be as high as possible, no more than one nautical mile, so the routes can take into account smaller scale temporal and geographical variations in both ocean and atmospheric data.

For a thorough explanation about optimal routing resolution, see Allsopp (1998).

6.3 Evaluation of averaged routes

The averaged routes way of making use of the ensembles seems to work quite well. We performed four averaged routes experiments, and in three of them the averaged routes performed better under uncertain weather scenarios than the route suggested by a single deterministic forecast (when comparing mean and median sailtimes). However, in the last experiment using wind ensemble and deterministic currents in the upwind case, the route suggested by the control forecast performed best. We believe that this is because the wind, as interpreted by the routing program, turns around through the south, so by following the averaged routes, the boat ends up spending to much time at unfavourable heading with the wind from a too tight angle. This could be avoided by giving the route less restrictions, so the boat can maintain its optimal upwind angles.

The route based on the mean positions performs better than the route based on the median positions in all the four cases, although it is only a slight improvement in the downwind case. By following the mean route, we follow a route that is probably not the most ideal for any of the weather scenarios, but it will perform well under all of them.

Chapter 7

Summary and final remarks

We consider whether ocean currents can play a decisive role when calculating optimal routes for sailboats given uncertainties in the weather forecast. During this work, a number of other relevant questions came up. The two most important are: 1) "Is there really a need for an ensemble for the ocean currents, or is one deterministic forecast sufficient?" 2) "How to best make use of weather and current ensembles in the routing process?"

In our approach to answer these questions, we created an ocean ensemble forecast. This was done by running the ROMS ocean model with different atmospheric forcing from the control and 20 ensemble members of LAMEPS. The ROMS model was run for the North Sea and Skagerrak area with a 4 km horizontal resolution, with 32 vertical sigma levels, resulting in an ocean ensemble forecast with a control and 20 ensemble members. Both forecasts has a lead time of 60 hours. The ocean ensemble was analyzed trough the calculation of average ensemble mean current speed, and the average ensemble standard deviation over the 60 hours. This was done to assess the uncertainty of the forecast. On the basis of the figure for average standard deviation (Figure 5.3 on page 29b), we selected 5 stations, and plotted timeseries for the development of both the wind and current ensembles at these stations (see Figure 5.4 through 5.13). The wind and current data was then converted to GRIB-format and used as input in a weather routing program to calculate optimal routes for a specific sailboat (in our case a Cookson 50, see Section 2.3.1). We performed four deterministic and eight probabilistic experiments in the routing program Expedition for a upwind case and a downwind case to analyse how the addition of currents affects the optimal routes.

The wind is the main source of energy driving the boat, while the current is more like a factor that, with a good knowledge about it, can be utilized to gain an advantage. It seems like in our situation with a uncertain weather forecast, that it is more important to know what is going on with

the wind than with the current. But as we show in the deterministic experiments, knowledge about the current conditions might give a significant gain in sailtime. Even though a 35 - 40 minutes ($1 - 1.5\%$) gain in sailtime might not seem like a lot, ocean races are sometimes won or lost by as little as a couple of minutes or even seconds. Taking into account that the average speed in these experiments is about 8.5 knots (410 nautical miles divided by 48 hours), 40 minutes would mean a distance of almost 6 nautical miles, or about 11 km! Currents can vary in speed and direction over short distances, on the open ocean often shorter distances than variations in the wind. A fascinating thought regarding this is that two boats sailing in the same area, with the same wind, could experience small differences in the current. If they experience a speed difference of as little as 0.01 knots in the current speed for one hour, this would result in a distance between the two boats of almost 20 meters. After 10 hours the difference would be as much as 185 meters! This kind of simple calculations are the main reason for our special interest in the importance of currents in the weather routing process for sailboats.

From the investigation we have done, we are confident to conclude that:

- Calculation of optimal routes for sailboats must include information about both wind and current conditions.
- In an uncertain weather situation, the addition of currents in the routing process can aid in the route selection process.
- For a medium long yacht race, like the one we have studied, there seems to be very little need for an ensemble forecasting system for the ocean.
- Weather routing based on ensemble forecasts is a valuable tool when the weather forecast is uncertain, and might prove to be an indispensable tool to calculate the safest route when the weather forecast is uncertain.

Ideally, an accurate forecast for both winds and ocean currents is necessary to do weather routing. As we showed in Figure 5.3 on page 29, there are regions that are less sensitive to variations in the atmospheric forcing. In these areas the forecast for the ocean currents are believed to be more accurate, whereas in the regions highly influenced by atmospheric forcing, the forecast is more uncertain when the weather forecast is uncertain.

We also note that there are times and regions where the current is more important than the wind when it comes to routing. We show that ocean current is a factor that can not be left out when calculating optimal routes for a sailboat. Even if it does not dominate in the routing process, it plays a decisive role in determining the fastest route, and thus should be included. In the upwind case, i.e. when sailing against the wind, there is

a significant difference in the routes in the beginning between the experiments using currents, and the one without (see Figure 5.16b). This indicates that the difference in current patterns in the Skagerrak area is more important than the differences in the wind. In the downwind case this difference is not that obvious by a simple visual examination of the routes in Figure 5.14, although it can be seen when examining the standard distances for the probabilistic experiments in Figure 5.19. One of the reasons for this is that the optimal routes based on wind input only, follows a very similar path to the routes that includes the currents. Also, the optimal routes enter the region of uncertain currents at slightly different times and places. Even though the difference in the location of the optimal routes in the downwind case are very small, the gain in sailtime when we include currents in the routing process is of the same order as in the upwind case. This shows that even small variations in the currents over small distances are important, and must be taken into account when calculating the fastest route.

In Section 5.4 we tested a technique we have developed for calculating a single optimal route based on an ensemble of weather input when the weather forecast is uncertain. The technique is based on the averaging of the optimal routes calculated in the routing program, using an ensemble of weather forecasts as input. The aim of this technique is to calculate a route that performs well under all the possible weather scenarios forecasted by the ensemble prediction system. Our effort resulted in producing the faster route in three out of four experiments, compared to following the route suggested by a single deterministic forecast. Ensemble forecasting is believed to play a major role in the methods used in weather forecasting as computational power increases in the years to come. Therefore it is important to find techniques to utilize the possibilities to use ensemble forecast within weather routing as this most likely will result in better routing. Although the method presented and used in this thesis needs refinement, and implementation into a weather routing program, this is an area worth further investigations.

7.1 Future work

The idea of implementing ensemble routing into a routing program is very interesting. The technique would need further development. The application we show in this thesis is only a first try.

It would be interesting to test these ideas and techniques on a longer route. For instance a crossing of the Atlantic would have been a very good test case to see how the ideas put forward here regarding probabilistic routing performs compared to deterministic weather input, which is the most

widespread technique used today. On a long race like crossing the Atlantic, the choices made early in the race will normally end up narrowing the range of options later in the race, and the ensemble routing technique could be helpful to ensure that options are open if something unexpected happens to the weather towards the end.

Also it is a intriguing thought to further develop the method so it could calculate routes for commercial ships based on criteria such as fuel consumption, avoiding areas of high waves and winds etc. Such a development would increase the benefits of ensemble prediction systems.

Bibliography

Albretsen, J. (2007). The impact of freshwater discharges on the ocean circulation in the Skagerrak/northern North Sea area. Part II: energy analysis. *Ocean Dynamics* (57), 287–304.

Albretsen, J. and L. P. Røed (2010). Decadal long simulations of mesoscale structures in the North Sea and Skagerrak using two ocean models. *Ocean Dynamics, In press*.

Allsopp, T. (1998, September). Stochastic weather routing for sailing vessels. Master's thesis, The University of Auckland, New Zealand.

Aspelien, T. (2008, December). Operational NORLAMEPS at Met.no. *HIRLAM Newsletter* (54), 88–91.

Bjerknes, W. (1904). Das Problem der Wettervorhersage betrachtet vom Standpunkte der Mechanik und der Physik. *Meteorologische Zeitschrift* (21).

Buizza, R. (2000). Chaos and weather prediction. *Meteorological Training Course Lecture Series*. (16.02.2010).

Driesenaar, T. (2009, March). General description of the HIRLAM model. `http://hirlam.org/index.php?option=com_content&view=article&id=64&Itemi%d=101`. (20.05.2010).

ECMWF (2010, February). ECMWF Products. `http://ecmwf.int/products/`. (20.05.2010).

Fossum, I. (2006, August). Analysis of instability and mesoscale motion off southern Norway. *JOURNAL OF GEOPHYSICAL RESEARCH 111*.

Haidvogel, D. B., H. Arango, W. P. Budgell, B. D. Cornuelle, E. Curchitser, E. Di Lorenzo, K. Fennel, W. R. Geyer, A. J. Hermann, L. Lanerolle, J. Levin, J. C. McWilliams, A. J. Miller, A. M. Moore, T. M. Powell, A. F. Shchepetkin, C. R. Sherwood, R. P. Signell, J. C. Warner, and J. Wilkin (2008, MAR 20). Ocean forecasting in terrain-following coordinates: Formulation and skill assessment of the Regional Ocean Modeling System. *JOURNAL OF COMPUTATIONAL PHYSICS 227*(7), 3595–3624.

Kalnay, E. (2003). *Atmospheric Modeling, Data Assimilation and Predictability*, Chapter 1.7 and Chapter 6. Cambridge University Press.

Lorenz, E. N. (1963). Deterministic non-periodic flow. *Journal of the Atmospheric Sciences 20*, 130–141.

Lorenz, E. N. (1965). A study of the predictability of a 28-variable atmospheric model. *Tellus 17*, 321–333.

Mathworks (2007). *MATLAB Help* (R2007b ed.). (16.02.2010).

Melsom, A. (2005). Mesoscale activity in the North Sea as seen in sensemble simulations. *Ocean Dynamics* (55), 338–350.

NCEP (1995, November). Ensemble forecasting at NCEP. `http://www.emc.ncep.noaa.gov/gmb/ens/info/ens_detbak.html`. (20.05.2010).

Nordborg, E. (2007, September). Sensitivity of a routing program to different weather input based on WRF simulations during offshore and near coastal navigation. Master's thesis, University of Oslo, Norway.

Persson, A. and F. Grazzini. *User Guide to ECMWF forecast products* (Version 4.0 ed.). ECMWF.

Røed, L. P. and I. Fossum (2004). Mean and eddy motion in the Skagerrak/northern North Sea: insight from a numerical model. *Ocean Dynamics* (54), 197–220.

Unden, P., L. Rontu, H. Järvinen, P. Lynch, J. Calvo, G. Cats, J. Cuxart, K. Eerola, C. Fortelius, J. A. Garcia-Moya, C. Jones, Geert, G. Lenderlink, A. Mcdonald, R. Mcgrath, B. Navascues, N. W. Nielsen, V. Degaard, E. Rodriguez, M. Rummukainen, K. Sattler, B. H. Sass, H. Savijarvi, B. W. Schreur, R. Sigg, and H. The (2002). HIRLAM-5 Scientific Documentation. Available at `http://citeseerx.ist.psu.edu/viewdoc/summary?doi=10.1.1.6.3794` (19.05.2010).

Appendix

Sourcecode for the averaged route calculation

We offer the sourcecode for the MATLAB-script used to calculate the averaged routes. The script takes the optimal routes exported from Expedition on csv-format as input. The route based on the control member should be named control.csv, and the routes based on the rest of the ensemble member should be named according to their ensemble member number.

```
%------------------------------------------------------------------
%
%       AVERAGE ROUTES
% Script that takes optimal routes as input, and calculates
% the average of those routes.
%
% (c) Nils Melsom Kristensen 2010
%------------------------------------------------------------------

close all
clear all
grey = [0.4,0.4,0.4];
green2 = [0,.5,0];
scrsz = get(0,'ScreenSize');
set(0,'DefaultFigurePosition', [0 0 scrsz(3) scrsz(4)],...
    'DefaultFigurePaperPositionMode','auto');
load coast
les = input(['How many ensemble members in addition to'...
             ' the control? ](default LAMEPS is 20) ');
if isempty(les)
    les=20;
end
timer=input('Number of trackpoints? (default is 44) ');
if isempty(timer)
    timer=44;
end
axesm('mercator','MapLatLimit',[53 59.1],'MapLonLimit',...
    [0 15],'Grid','on','Frame','on','MeridianLabel',...
    'on','ParallelLabel','on')
geoshow(lat,long,'DisplayType','polygon')
```

```
31
32 %Control
33 filename=['data/control.csv'];
34 [UTC, TwdM{1}, G, Tws{1}, Twa, Targ, Bsp, Sail, CrsM,...
35     MSLP, Rain,Latitude1, Latitude2, Latitude3,...
36     Longitude1, Longitude2,Longitude3] = ...
37     textread(filename, ...
38     '%s %3f %s %f %s %s %s %s %s %s %s %d %6s %s %d %6s %s',...
39     timer, 'delimiter' , ',', 'headerlines', 1);
40 for j=1:1:timer,
41     latnum=str2num(Latitude2{j});
42     lonnum=str2num(Longitude2{j});
43     lattt(j)=Latitude1(j)'+(latnum./60);
44     lonnn(j)=Longitude1(j)'+(lonnum./60);
45 end
46 latt=lattt';
47 lonn=lonnn';
48 waypoints{1}=[latt lonn];
49 [lttrk,lntrk] = track('rh',waypoints{1},'degrees');
50 geoshow(lttrk,lntrk,'DisplayType','line','color','k',...
51     'LineWidth',2)
52
53
54 for i=1:1:les,
55     filename=['data/' num2str(i) '.csv'];
56     [UTC, TwdM{i+1}, G, Tws{i+1}, Twa, Targ, Bsp, Sail,...
57         CrsM, MSLP, Rain, Latitude1, Latitude2, Latitude3,...
58         Longitude1, Longitude2, Longitude3] = ...
59         textread(filename, ...
60         '%s %3f %s %f %s %s %s %s %s %s %s %d %6s %s %d %6s %s',...
61         timer, 'delimiter' , ',', 'headerlines', 1);
62     for j=1:1:timer,
63         latnum=str2num(Latitude2{j});
64         lonnum=str2num(Longitude2{j});
65         lattt(j)=Latitude1(j)'+(latnum./60);
66         lonnn(j)=Longitude1(j)'+(lonnum./60);
67     end
68     latt=lattt';
69     lonn=lonnn';
70     waypoints{i+1}=[latt lonn];
71     [lttrk,lntrk] = track('rh',waypoints{i+1},'degrees');
72     %geoshow(lttrk,lntrk,'DisplayType','line','color',grey,...
73     %'LineWidth',1)
74 end
75
76
77
78 %Calculate mean route.....
79 antallruter=les+1;
80 latmean(1:timer)=0.0;
81 lonmean(1:timer)=0.0;
82 for i=1:1:timer,
83     for j=1:1:antallruter,
84         lattemp(j)=waypoints{j}(i,1);
85         lontemp(j)=waypoints{j}(i,2);
```

```
86          [latmean(i),lonmean(i)] = meanm(lattemp',lontemp');
87      end
88      dist(i)=stdist(lattemp',lontemp');
89      [latstd(i),lonstd(i)]=stdm(lattemp',lontemp');
90  end
91  geoshow(latmean,lonmean,'DisplayType','line','color','r',...
92      'LineWidth',2)
93  %-----Mean route
94  [lttrk,lntrk] = track('rh',waypoints{1},'degrees');
95  geoshow(lttrk,lntrk,'DisplayType','line','color','k',...
96      'LineWidth',2)
97  %-----Median route
98  for i=1:1:timer,
99      for j=1:1:antallruter,
100         templat(j)=waypoints{j}(i,1);
101         templon(j)=waypoints{j}(i,2);
102     end
103     medianlat(i)=median(templat(:));
104     medianlon(i)=median(templon(:));
105 end
106 geoshow(medianlat,medianlon,'DisplayType','line','color',...
107     'b','LineWidth',2)
108 %-----
109 meanroute=[1:timer; latmean; lonmean]';
110 medianroute=[1:timer; medianlat; medianlon]';
111 course_dist=legs(latmean,lonmean);
112 csvwrite('csv/meanroute.csv',meanroute);
113 kmlwrite('kml/mean.kml',latmean,lonmean);
114 csvwrite('csv/medianroute.csv',medianroute);
115 kmlwrite('kml/median.kml',medianlat,medianlon);
116 csvwrite('csv/course_dist_mean.csv',course_dist);
117 dist=deg2nm(dist).*cosd(latmean);
118 csvwrite('../geostddev_nocurr.csv',dist);
119
120
121 close all
```